



A model for jet dispersion in a congested environment

Prepared by
Advantica Technologies Limited
for the Health and Safety Executive

CONTRACT RESEARCH REPORT
396/2001



A model for jet dispersion in a congested environment

M G Cooper
Advantica Technologies Limited
Ashby Road
Loughborough
Leicestershire
LE11 3GR
United Kingdom

This report addresses the problem posed by the interaction of a gas jet when it encounters obstacles which when taken together can be construed as a congested environment. The aim of the project was to take an existing integral model normally applied to level, unobstructed terrain as a basis for modelling in more realistic situations. Semi-empirical methods were used to account for dilution effects and the new model applied to pre-existing data. The model is suitable for prediction of concentrations down to about 1% of the source concentration and would therefore not be suitable for toxic releases where there could still be significant harm at much lower concentrations.

This report and the work it describes were funded by the Health and Safety Executive (HSE). Its contents, including any opinions and/or conclusions expressed, are those of the author alone and do not necessarily reflect HSE policy.

© Crown copyright 2001

Applications for reproduction should be made in writing to:
Copyright Unit, Her Majesty's Stationery Office,
St Clements House, 2-16 Colegate, Norwich NR3 1BQ

First published 2001

ISBN 0 7176 2234 7

All rights reserved. No part of this publication may be reproduced, stored in a retrieval system, or transmitted in any form or by any means (electronic, mechanical, photocopying, recording or otherwise) without the prior written permission of the copyright owner.

Contents

1	INTRODUCTION	1
2	FREE JET DISPERSION	2
2.1	EXISTING JET DISPERSION MODEL.....	2
2.2	EXTENSION TO THREE DIMENSIONS	4
2.3	VERIFICATION.....	5
3	INTERACTION WITH OBSTACLES	7
3.1	INTRODUCTION	7
3.2	MOMENTUM EFFECTS.....	8
3.3	DILUTION EFFECTS.....	9
3.4	LARGE OBSTACLES	10
3.5	ANGLED INTERACTION	10
3.6	IMPLEMENTATION.....	11
4	VALIDATION	15
4.1	ADVANTICA DATA	15
4.2	SHELL DATA	19
4.3	JIP DATA	21
5	DISCUSSION	28
6	REFERENCES	29
	NOMENCLATURE	30
A	Appendix – User guide	A-1

Executive Summary

Following a submission by Advantica (then BG Technology) to the HSE in 1999 under the Competition for Ideas, the HSE contracted Advantica to develop a model for jet dispersion in a congested environment. This report is a record of the work carried out by Advantica under the contract, describing the development and validation of the model.

1 INTRODUCTION

Over the years, a number of models have been developed for the dispersion of jet releases in an atmospheric crossflow. This has included a number of integral models, using simple entrainment relationships to describe the rate at which the jets are diluted by air. However, these models are generally only applicable to releases over level, unobstructed terrain. In reality, many of the releases that might occur on industrial plant would inevitably encounter some form of obstacle.

Following a submission by Advantica (then BG Technology) to the HSE in 1999 under the Competition for Ideas, the HSE contracted Advantica to develop a model for jet dispersion in such a congested environment.

The aim of the project was to use an existing integral model for jet dispersion over unobstructed terrain as the basis for the development of a model for dispersion in a realistic onshore process or storage site. Simple, semi-empirical methods were to be produced to account for the dilution effects resulting from jet interaction with one or more obstacles. This has now been completed successfully and this report provides an account of the work carried out to meet the objectives. The method that has been developed for doing this is based on a similar simple approach that has been successfully employed by Advantica for predicting the dispersion of specific types of releases in an offshore environment and of denser-than-air gas clouds on an industrial site, although the form of the relationships used are not the same.

The overall intention of the programme of work is to demonstrate that a relatively simple integral-type model can be used to predict the bulk effects of jet interaction with simple obstacle configurations, rather than to develop a finished tool with graphical interfaces.

The work commenced in June 2000 and was originally scheduled for completion by the end of May 2001. The final completion date was subsequently delayed until July 2001 by agreement with HSE.

The model as described in this report is designed for predicting dispersion to concentrations of the order of 1% of the source concentration, and as such would not be suitable for some toxic releases where much greater degrees of dilution may be of interest. Note that although this report refers in various places to dispersion distances to the lower flammable limit (LFL), this should not be taken to imply that such calculations are necessarily indicative of the maximum extent of the flammable hazard range in any particular case.

2 FREE JET DISPERSION

2.1 Existing jet dispersion model

The basis of the development work in this project is the existing jet dispersion model JINX [1] which was developed by Advantica, although the principles described in this report could be applied to any similar dispersion model. JINX provides a simple, straight-forward and well-validated tool which is routinely used for assessing the safety of venting systems and for the dispersion of accidental releases from high pressure pipework. JINX is an integral-type mathematical model which predicts the bulk trajectory and dilution of a gaseous jet for a wide range of source gas properties and conditions (i.e. molecular weight, pressure and temperature) and atmospheric conditions. The program uses the mass flow rate of the release and the orifice diameter to determine whether the release is sonic or sub-sonic. In either case, it takes account of compressibility effects in calculating the initial momentum flux. Mass, momentum, species and enthalpy conservation equations are then solved for the total fluxes in the jet. JINX also incorporates ground interaction effects which are important for horizontal releases near ground level. It has been validated using the results of extensive field-scale and wind tunnel trials carried out by Advantica. The model is described in detail in [1] and the co-ordinate system used by JINX is shown in Figure 1.

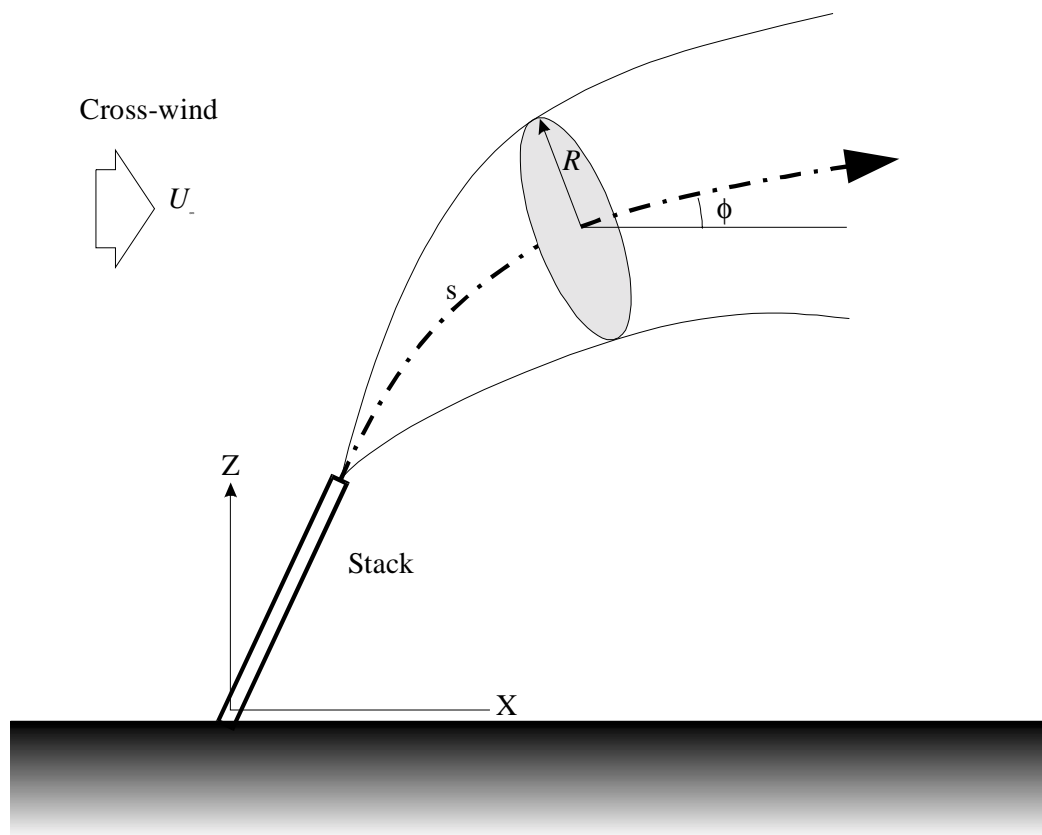


Figure 1: Co-ordinate system for two-dimensional jet model

The main equations solved by JINX are summarised below (see Section 7 for definition of symbols):

Conservation of mass

$$\frac{d}{ds} \dot{M} = E \quad (1)$$

Conservation of momentum

$$\frac{d}{ds} W_H = E.U_\infty - D_x \quad (2)$$

$$\frac{d}{ds} W_v = -\pi.R^2.g(\rho - \rho_\infty) \quad (3)$$

Conservation of species

$$\frac{d}{ds} (\dot{M}.c_M) = 0 \quad (4)$$

Conservation of enthalpy

$$\frac{d}{ds} H = \frac{E(H_\infty - H)}{\dot{M}} \quad (5)$$

Entrainment

$$E = E_1 + E_2 + E_3 \quad (6)$$

where

$$E_1 = \alpha_1.2\pi\rho_\infty \sqrt{\frac{|(W - W_\infty)|}{\pi\rho_\infty}} \quad (7)$$

$$E_2 = \alpha_2.2\pi R\sqrt{(\rho.\rho_\infty)}.U_\infty |\sin \phi| \quad (8)$$

$$E_3 = \alpha_3.\rho_\infty.V_\infty \quad (9)$$

A similar set of equations, but with the addition of gravity-driven lateral spreading when appropriate, is solved in the event of the jet interacting with the ground.

The main limitation of the existing version of JINX is that it is restricted to two dimensions, *i.e.* releases in the plane of the wind, as the model was originally designed for worst-case hazard analysis. In order that the model is able to interact

with a complex array of obstacles, it is first necessary to extend the free jet model so that it is fully three-dimensional.

2.2 Extension to three dimensions

The co-ordinate system for releases in three dimensions is shown in Figure 2.

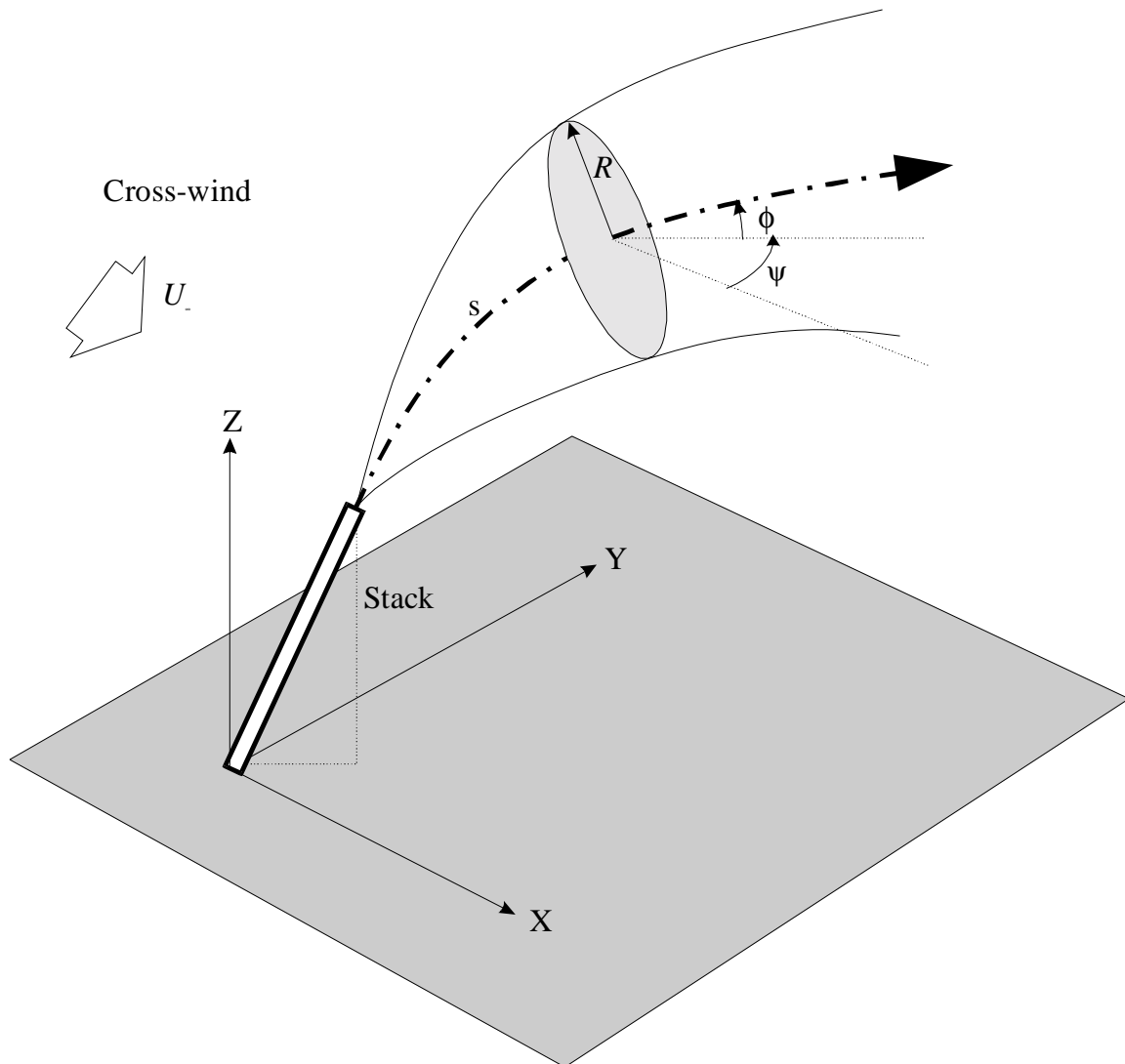


Figure 2: Co-ordinate system for three-dimensional jet model

When extended to three dimensions, the equations solved by JINX are as follows:

Conservation of mass

$$\frac{d}{ds} \dot{M} = E \quad (10)$$

Conservation of momentum

$$\frac{d}{ds} W_x = E U_\infty - D_x \quad (11)$$

$$\frac{d}{ds} W_y = -D_y \quad (12)$$

$$\frac{d}{ds} W_v = -\pi R^2 \cdot g (\rho - \rho_\infty) \quad (13)$$

Conservation of species

$$\frac{d}{ds} (\dot{M} \cdot c_M) = 0 \quad (14)$$

Conservation of enthalpy

$$\frac{d}{ds} H = \frac{E(H_\infty - H)}{\dot{M}} \quad (15)$$

Entrainment

$$E = E_1 + E_2 + E_3 \quad (16)$$

where

$$E_1 = \alpha_1 \cdot 2\pi \rho_\infty \sqrt{\frac{|(W - W_\infty)|}{\pi \rho_\infty}} \quad (17)$$

$$E_2 = \alpha_2 \cdot 2\pi R \sqrt{(\rho \cdot \rho_\infty)} \cdot U_\infty \sqrt{1 - \cos^2 \phi \cos^2 \psi} \quad (18)$$

$$E_3 = \alpha_3 \cdot \rho_\infty \cdot v_\infty \quad (19)$$

2.3 Verification

A number of checks have been made in order to verify that the modified equations (10) – (19) are implemented correctly in the three-dimensional free jet model. Firstly, a series of runs were made for releases in the plane of the wind, and the results compared directly with the results of the two-dimensional free jet model for a range of release directions, flowrates and windspeeds. Secondly, comparisons were made between vertical and horizontal releases in three dimensions, since these should yield very similar results for a flat wind profile provided that the release is such that buoyancy and ground effects are unimportant. An example of such a comparison is shown in Figures 3 and 4. Figure 3 shows the predicted trajectory as far as the LFL for a range of release directions in the vertical plane and Figure 4 shows

corresponding trajectories for releases in the horizontal plane, in both crosswind directions.

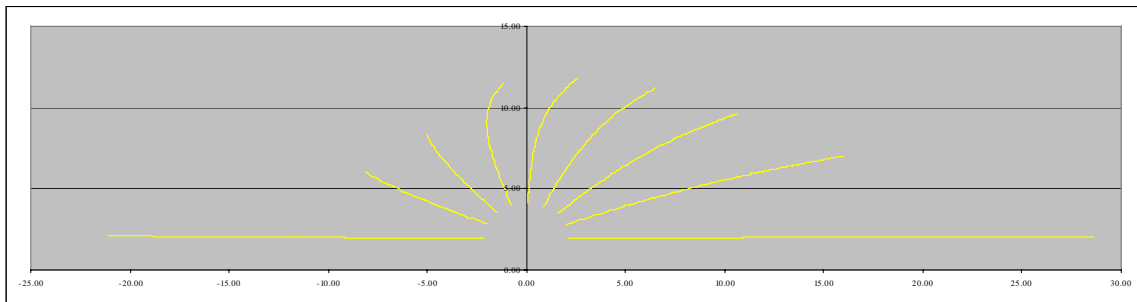


Figure 3: Predicted jet trajectories to LFL for releases in the vertical wind plane

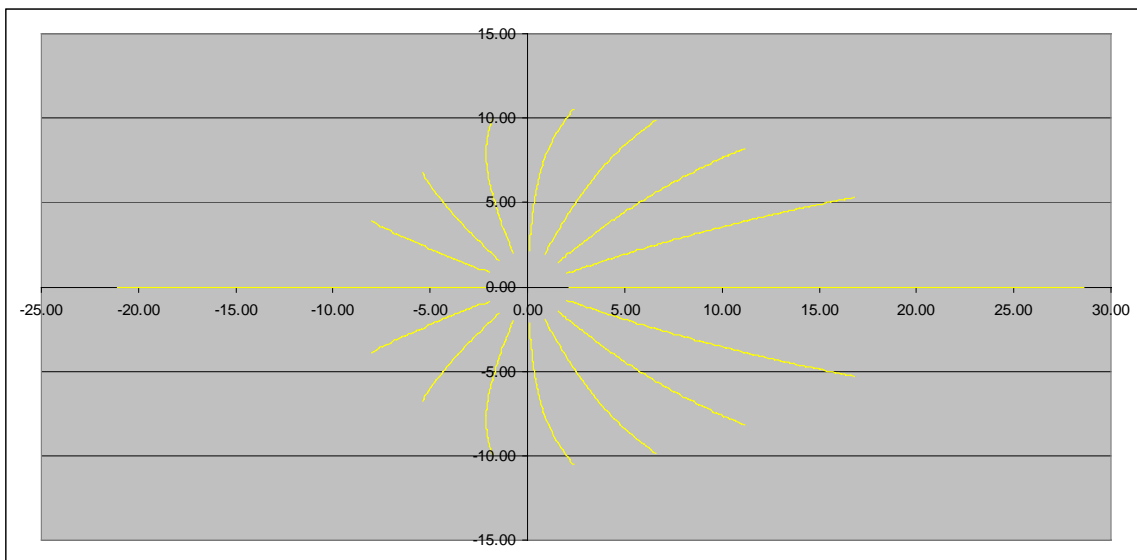


Figure 4: Predicted jet trajectories to LFL for releases in the horizontal plane

It can be seen that the trajectories for the vertical and horizontal releases are very similar, and that the results for horizontal releases between 0 and 180 degrees are an exact mirror image of those between 180 and 360 degrees. Whilst such comparisons cannot provide conclusive evidence that the coding is performing exactly as intended, a number of such comparisons taken together do give a degree of confidence in the validity of the model implementation.

3 INTERACTION WITH OBSTACLES

3.1 Introduction

The flow-field resulting from the interaction of a high-momentum jet with obstacles is highly complex and requires the use of sophisticated computational fluid dynamic techniques in order to resolve the details of the flow. However, for hazard analysis purposes, it is seldom necessary to resort to such methods, since in many instances, the ultimate aim is to estimate the variation of bulk parameters, such as concentration with distance or time. As a result, it is desirable to be able to model such interactions in a global, semi-empirical manner using simple integral-type models such as the jet dispersion model describe in Section 2. Naturally, such an approach would not be expected to predict the details of the flow in the wake immediately behind an obstacle, but should be accurate enough to estimate the downstream dispersion to concentrations of the order of the LFL.

The types of obstacle likely to be encountered on a process site can generally be categorised as one of the following:

- Cylinders, e.g. pipes and storage tanks
- Rectangular boxes, e.g. buildings, storage tanks and steelwork
- Flat plates, e.g. floors and steelwork

The JINX model is already able to account of the jet grounding on a flat surface by reducing entrainment along the bottom edge and incorporating gravity slumping.

As an added simplification, flat plates could be considered as special types of thin boxes, thus reducing the number of obstacle types to two.

On a process site, any such obstacles are likely to be oriented vertically or horizontally, but bearing in mind that a release could occur in any direction, the following obstacle orientations will be considered here:

- Vertical
- Horizontal, at any angle

From experimental observation, it can be postulated that the effects of obstacles on the dispersion of high momentum jets are two-fold:

1. A loss in the forward momentum of the jet which arises through frictional losses as fluid passes the obstacle and also through the generation of turbulence in the wake of the obstacle,
2. As a consequence of the increased turbulence, the overall entrainment rate of ambient fluid into the jet increases, resulting in faster dilution.

Modelling each of these two effects is considered in the following two sections for jets which impact normal to the obstacle. The effects of very large obstacles and oblique interaction are considered in Sections 3.4 and 3.5 .

3.2 Momentum effects

It is proposed that the proportion of momentum lost by the jet is dependent on the relative size of the jet and obstacle cross-sections, so that the momentum terms immediately after passing the obstacle take the following form:

$$W'_x = W_x \cdot f \quad (20)$$

$$W'_y = W_y \cdot f \quad (21)$$

$$W'_v = W_v \cdot f \quad (22)$$

where the parameter f is defined as follows:

$$f = \frac{K}{\left(K + \frac{A_{obs}}{A_{jet}} \right)} \quad (23)$$

The effective jet area, A_{jet} , is the cross sectional area of the jet, as calculated from the bulk flow parameters, and A_{obs} is the area of the obstacle which interacts with the jet, which is defined in Figure 5. The parameter K depends on the shape of the obstacle and is defined in terms of a drag coefficient C_d :

$$K = \frac{2}{C_d} \quad (24)$$

The value of C_d has been assumed to be 0.3 for cylindrical obstacles and 0.6 for box-type obstacles (see Section 4). Values for other shapes could be determined by experiment.

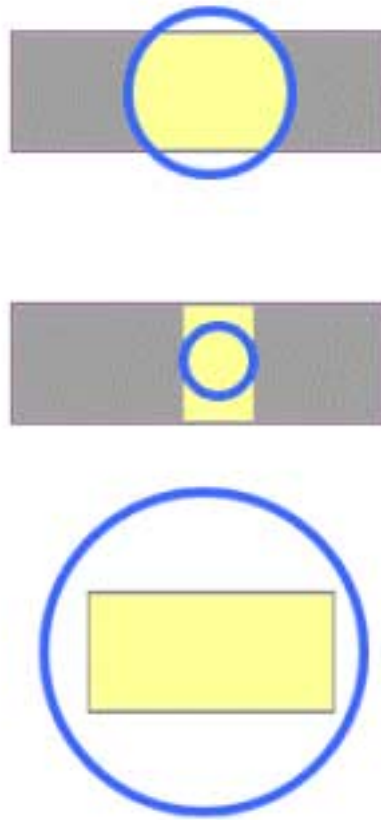


Figure 5: Illustration of effective obstacle area for three different cases: (top) jet larger than obstacle diameter, but smaller than obstacle length; (middle) jet smaller than both obstacle dimensions; (bottom) jet larger than both obstacle dimensions. Jet cross-section shown in blue, obstacle in grey, effective obstacle area in yellow.

3.3 Dilution effects

The increased dilution of the jet in the obstacle wake is accounted for by enhancing the entrainment coefficient for entrainment due to momentum shear (α_1 in Equation 17). The degree to which the entrainment coefficient is enhanced depends on the same area interaction parameter used for the momentum loss calculation in Section 3.2:

$$\alpha_1' = \alpha_1 + 0.9 \cdot \left(\frac{A_{obs}}{A_{jet}} \right) \cdot (0.2 - \alpha_1) \quad (25)$$

By this mechanism, the entrainment coefficient is increased from its base value of 0.07 up to a maximum of 0.2. Note that the enhanced entrainment continues to be applied for all time once an obstacle has been hit, and that interaction with additional

obstacles augments the entrainment coefficient still further (up to its maximum value). This methodology agrees with experimental evidence for dispersion to concentrations of the order of the LFL, but some downstream decay of this effect may be considered necessary if one is considering, for example, the dispersion of toxic releases down to much lower concentration levels.

3.4 Large obstacles

The methodology described in Sections 3.2 predicts that as the size of the obstacle relative to the jet increases, so the momentum loss continues to increase. In reality, however, there will be a point at which the jet will effectively stall if it impacts normal to the obstacle (angled interactions are dealt with in the following section). We assume that the jet continues to make forward progress as long as the following relationship is true :

$$\frac{D_{obs}}{D_{jet}} < \frac{2.4}{C_d} \quad (26)$$

The constant on the right hand side of equation (26) is an estimate based on the available data, but ideally would be determined by specific experiments. The chosen value of 2.4 means that for a cylinder, the jet would be completely stopped by an obstacle with a diameter greater than eight times the jet diameter, or four times the jet diameter for a rectangular obstacle. If the dispersion calculation needs to be continued past this point, then the results from the jet calculation to this location could be used to determine the initial conditions for a fan or wall jet calculation, or for a passive dispersion calculation if distances further downstream are of interest.

3.5 Angled interaction

When considering a release of gas on a real site, as opposed to an idealised experiment, the most likely occurrence would be a jet interacting an oblique angle to the obstacle. In the absence of experimental data, we would intuitively expect that the entrainment enhancement term in equation (25) would take the following form:

$$\alpha_1' = \alpha_1 + 0.9 \cdot \left(\frac{A_{obs}}{A_{jet}} \right) \cdot (0.2 - \alpha_1) \cdot \sin \theta \quad (27)$$

where θ is the angle between the jet axis and the obstacle axis. No modification is made to the momentum loss term in equation (23) for angled interaction.

For large oblique obstacles (i.e. when the relationship in equation (26) is no longer true), rather than stalling, the jet is likely to be deflected. Large obstacles are deemed to be at an oblique angle when the horizontal angle between the jet axis and the obstacle axis is less than about 10 degrees. When this occurs, the momentum terms in equations (11) to (13) are re-aligned so that the jet momentum component normal to the obstacle is directed along the obstacle axis, with no overall momentum losses.

3.6 Implementation

The logic for determining whether the jet is likely to interact with an obstacle in three dimensions is not trivial. This logic also has to be integrated with the existing logic within the model for detection of the jet interacting with the ground. The overall flowchart for detecting jet interaction with obstacles and/or the ground is shown in Figure 6. The logic for determining whether an obstacle has been passed on the current step (required as part of the flowchart in Figure 6) is shown in Figure 7. Similar logic charts have been produced for the behaviour of the jet in the event of interaction with the ground (the stopping point for the flowchart in Figure 6), but have not been included in this report for simplicity. Note that these logic charts relate specifically to the implementation of the impacting jet methodology in the Advantica jet dispersion model. Incorporation of the methodology into other models may require a very different approach, depending on the code structure and on the solution schemes employed.

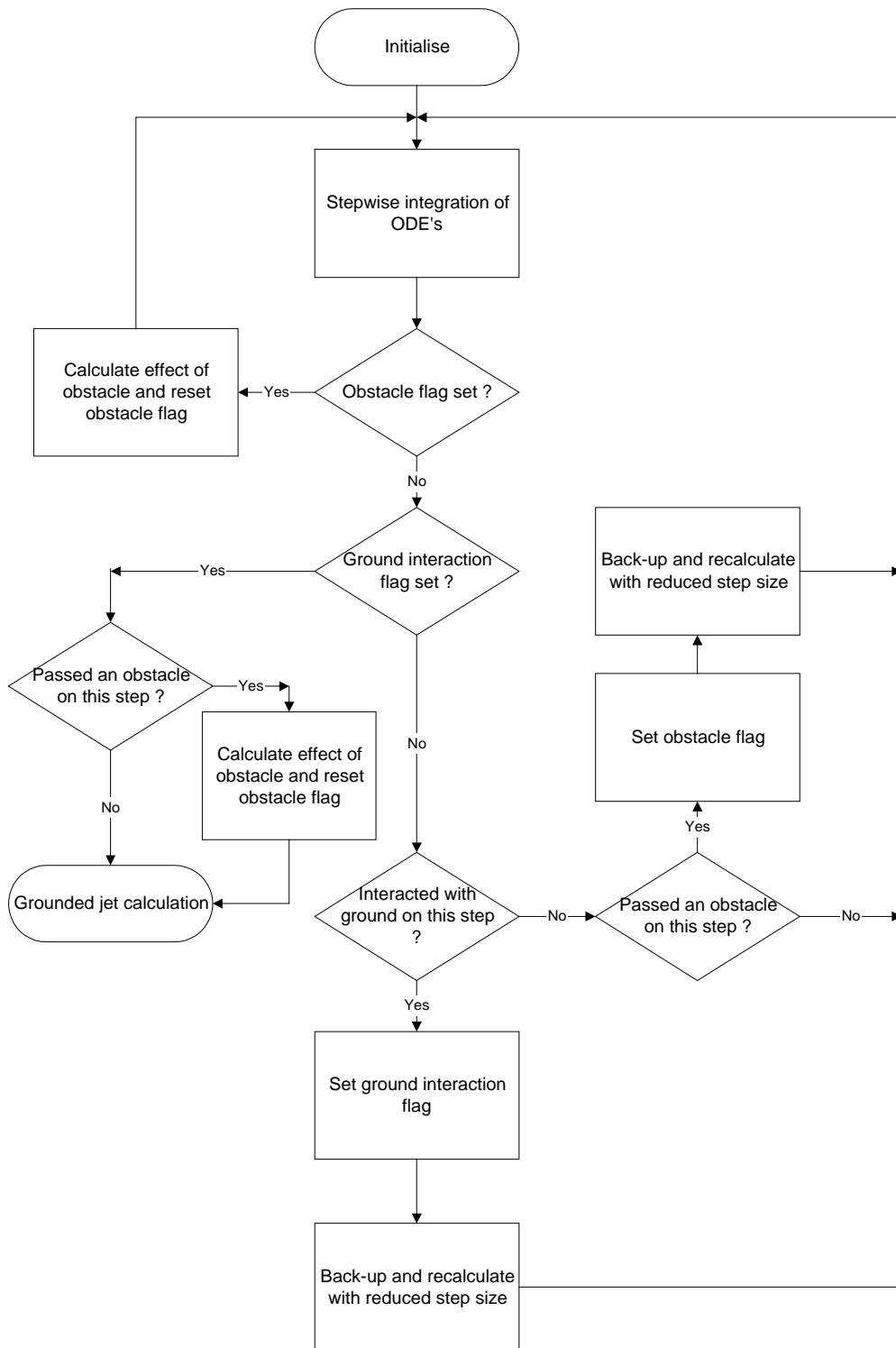


Figure 6: Strategy for jet interaction with obstacles and ground

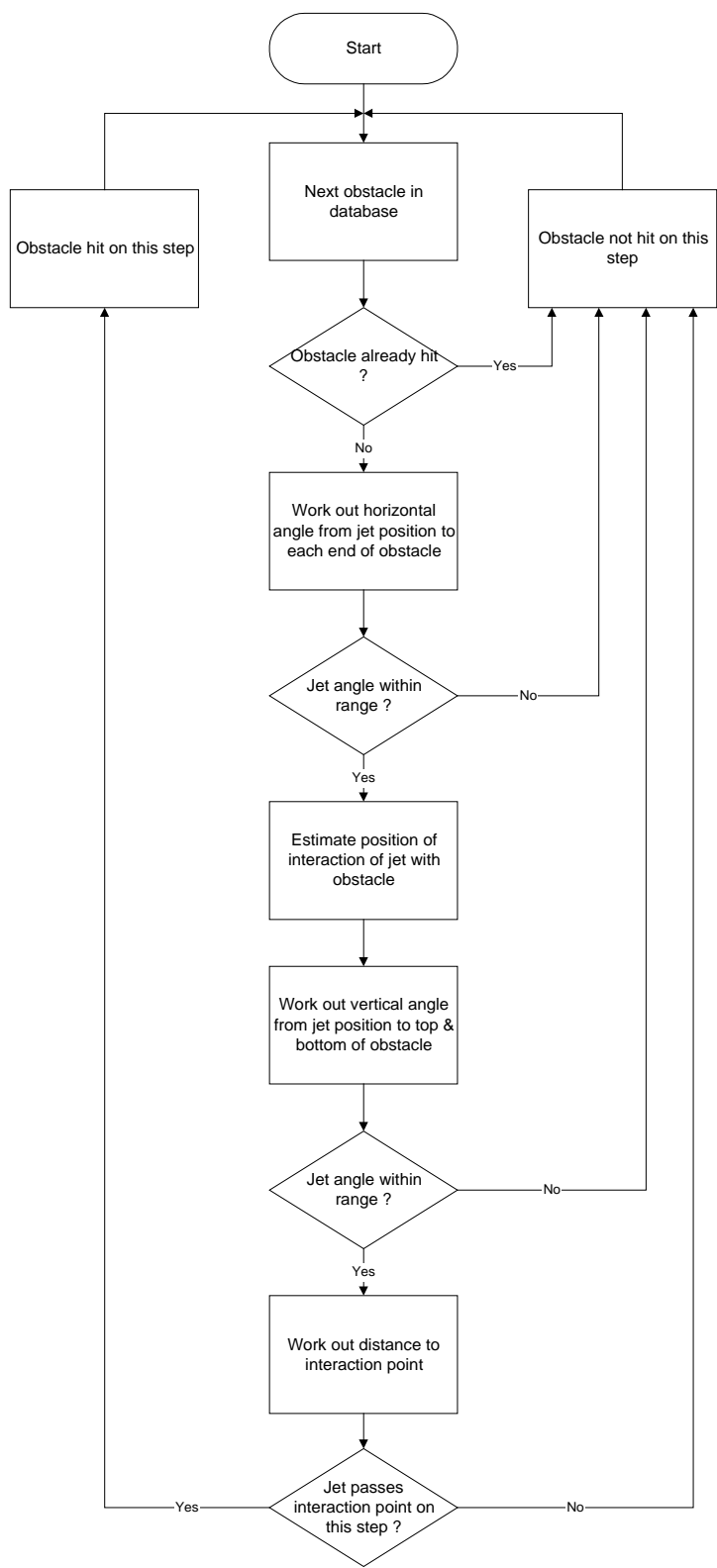


Figure 7: Strategy for determining which obstacles are hit by jet

The following information is required for each obstacle that the jet interacts with:

- Co-ordinates of one end of obstacle (m).
- Orientation with respect to down-wind axis (deg.) (For horizontal obstacles only).
- Obstacle diameter or width (m).
- Obstacle length (m).
- Obstacle shape identifier.

The formats of the input data files for the jet dispersion model and the obstacle data are described in Appendix A of the report, together with detailed instructions for running the model. Example input and output files are also listed.

4 VALIDATION

Extensive literature searches have revealed very little experimental data relevant to the effect of obstacles on the dispersion of momentum-dominated gas jets. The bulk of published work on the interaction of releases with obstacles has been related to dense gases at low velocities. However, three sources of data have been identified and these are described and compared with the predictions of the revised jet dispersion model in the remainder of this section. The graphs presented in this section (Figures 8-15 and 19-24) show concentration as a function of downwind distance, with the experimental measurements shown as red points, and the predictions of the model as a yellow line. For comparison purposes, the free jet prediction (*i.e.* no effect of obstacles included) is shown as a blue line. The position and width of the obstacle is marked in grey.

4.1 *Advantica data*

Advantica have carried out a series of wind-tunnel tests in which natural gas was released horizontally and impacted onto single cylindrical obstacles of various diameters. The length of the obstacles was very much longer than the diameter of the jet and the obstacles were positioned so that they were perpendicular to the jet direction. The release rate was 0.011 kg/s through a 10.7 mm diameter nozzle, corresponding to a release velocity of 156 m/s. Gas concentrations were measured at a number of locations downstream of the obstacle using aspirating probes. The results from two configurations were published [2], but additional unpublished data was also obtained for obstacles with smaller diameters.

Figures 8 and 9 show comparisons for the jet impacting with an obstacle of diameter 150 mm at downstream distances of 157 mm and 630 mm respectively. The figures show good agreement with the data once the wake region behind the obstacle has been passed (about 4 or 5 obstacle diameters downstream). They also demonstrate the significant effect that the obstacle has on the concentration levels when compared with the free jet case. These two data sets were used in the calibration of the model for interaction with cylindrical obstacles.

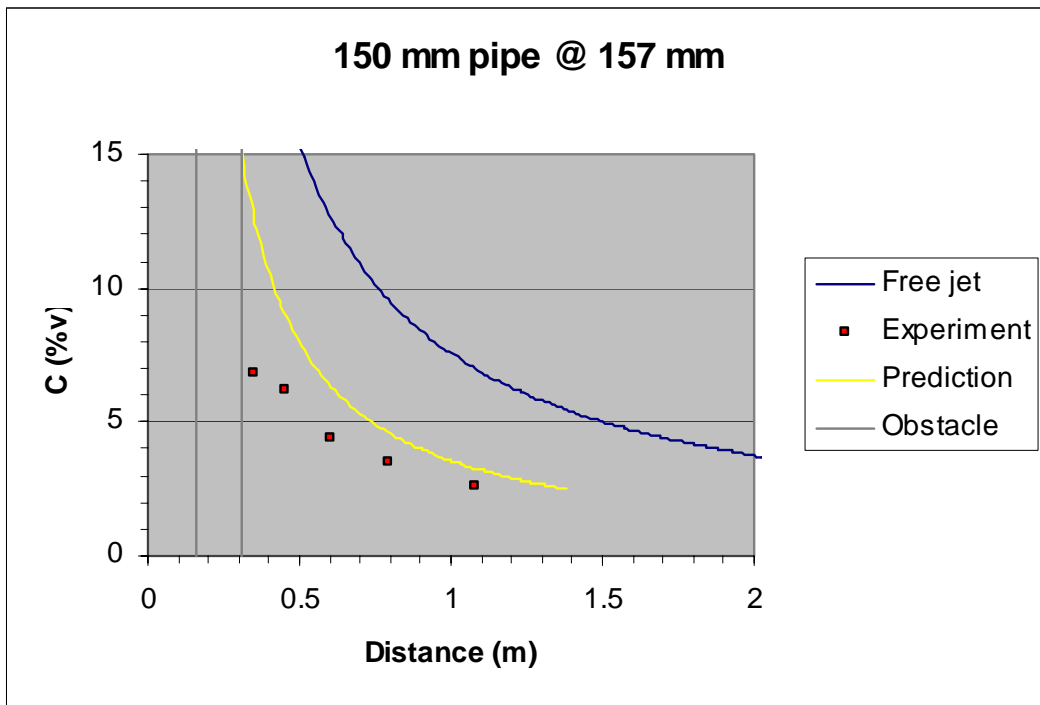


Figure 8: Concentration as function of downstream distance for jet hitting 150 mm diameter obstacle at distance of 157 mm

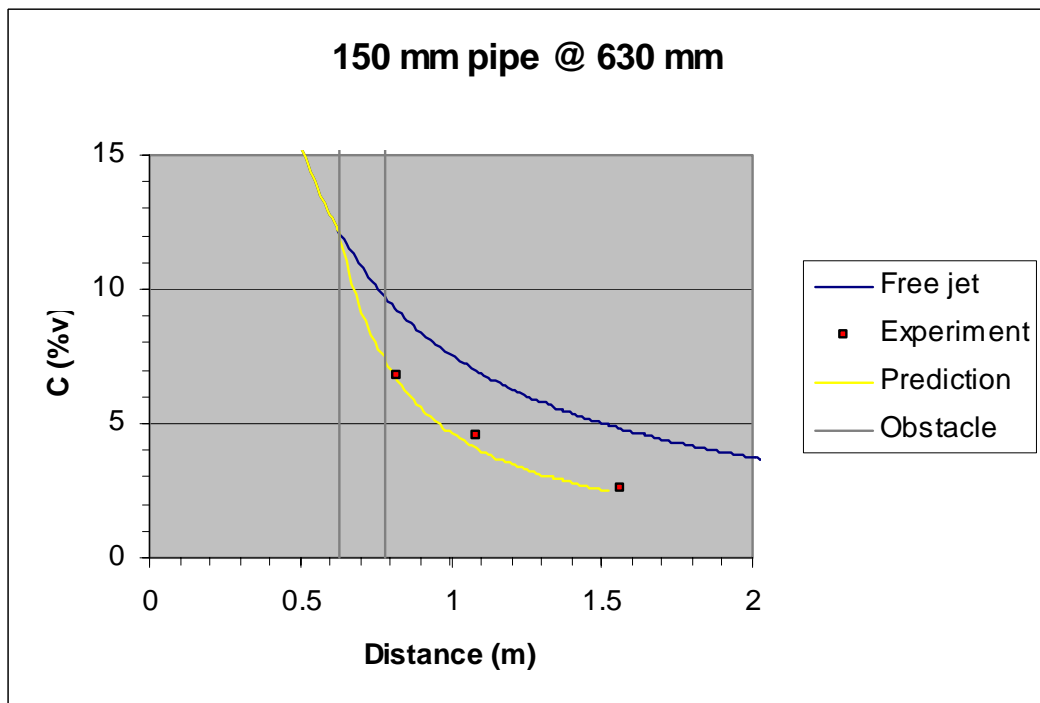


Figure 9: Concentration as function of downstream distance for jet hitting 150 mm diameter obstacle at distance of 630 mm

Figures 10 to 12 show similar comparisons for obstacle diameters of 100 mm, 50 mm and 25 mm. These demonstrate levels of agreement which are almost as good as for the 150 mm diameter obstacle, but represent a more onerous test as they were not used in the model calibration.

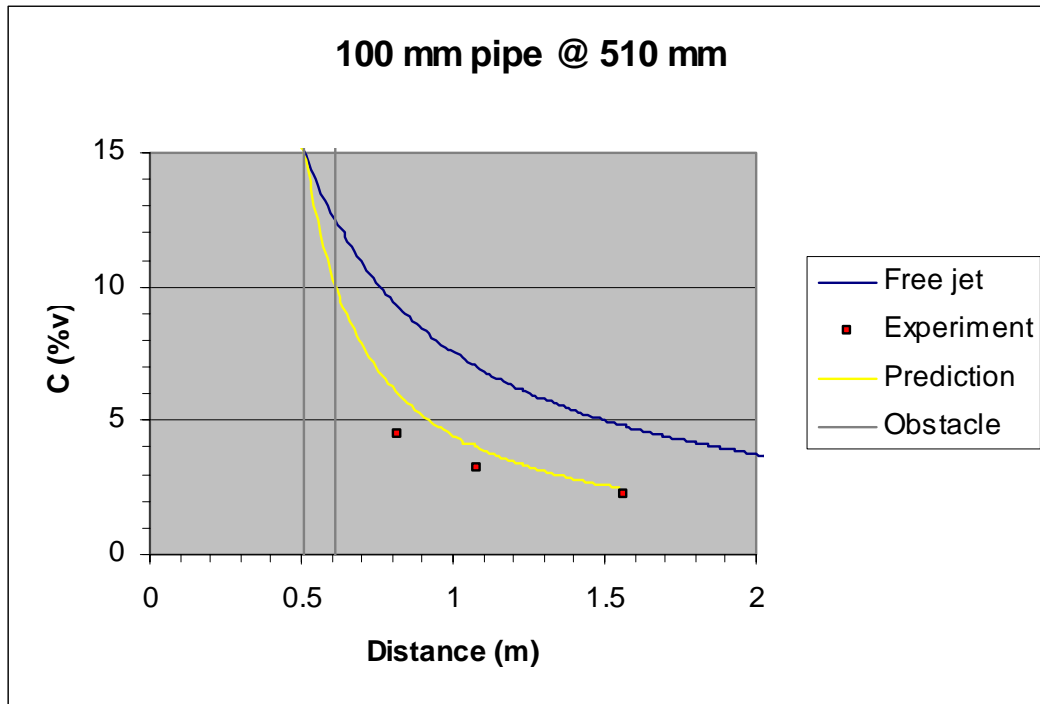


Figure 10: Concentration as function of downstream distance for jet hitting 100 mm diameter obstacle at distance of 510 mm

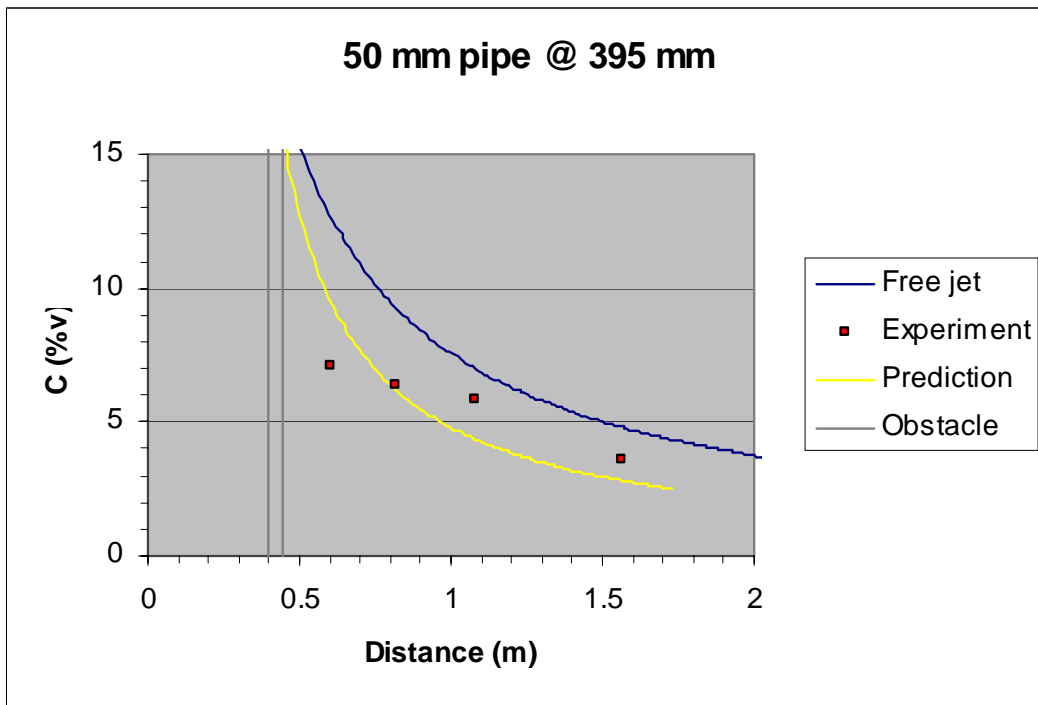


Figure 11: Concentration as function of downstream distance for jet hitting 50 mm diameter obstacle at distance of 395 mm

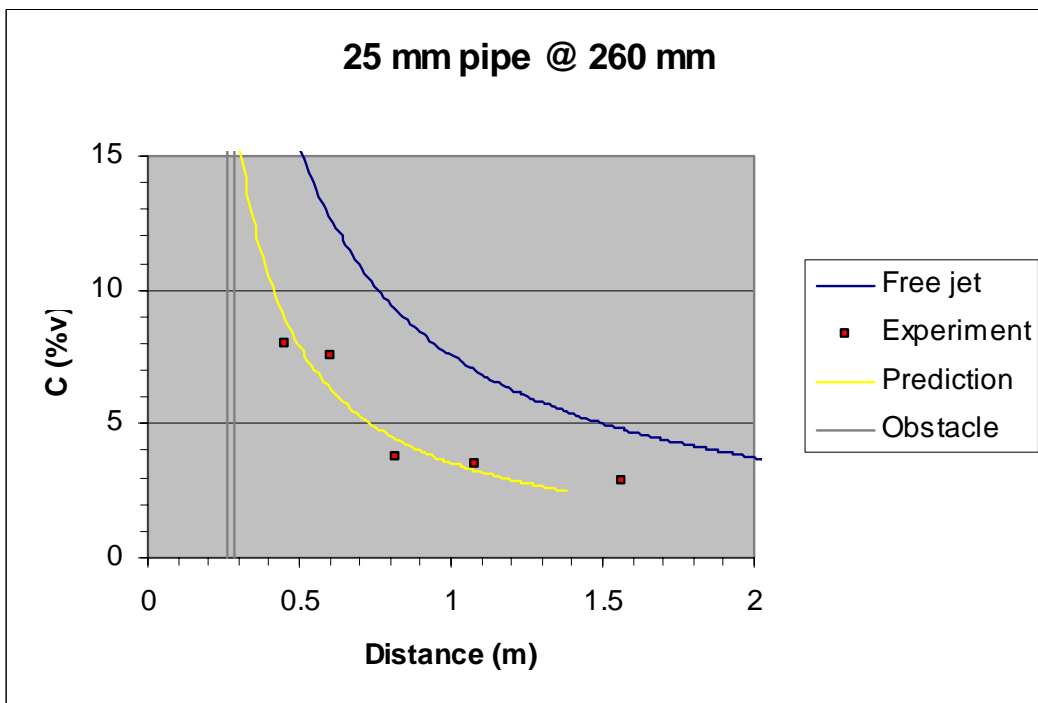


Figure 12: Concentration as function of downstream distance for jet hitting 25 mm diameter obstacle at distance of 260 mm

4.2 Shell data

At about the same time as the Advantica work was being carried out, Shell published data from very small scale experiments [3] in which seeded nitrogen was released in zero-wind conditions from a 2 mm diameter nozzle. The release rate was 7.5×10^{-5} kg/s, corresponding to an exit velocity of just 20 m/s and a Reynolds number of 2700 (i.e. barely turbulent). Gas concentrations were measured for flat and cylindrical obstacles using laser-induced fluorescence. Bryce & Fryer-Taylor's paper states that further experiments were conducted at exit velocities of up to 60 m/s, but these do not appear to have been published.

In Figure 13, a 5 mm diameter cylindrical obstacle was positioned perpendicular to the jet flow direction at 25 mm from the release point. Good agreement is again found once the jet has progressed beyond the wake region immediately behind the obstacle.

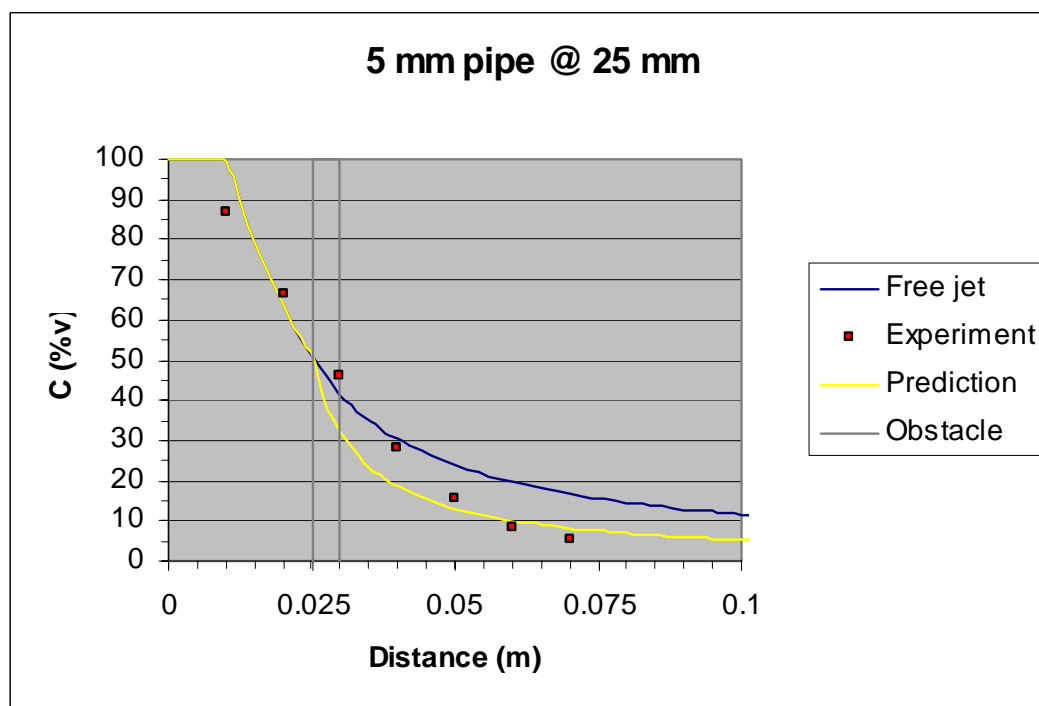


Figure 13: Concentration as function of downstream distance for jet hitting 5 mm diameter obstacle at distance of 25 mm

In Figure 14, a flat plate of width 5 mm was positioned perpendicular to the jet flow direction at 25 mm from the release point.

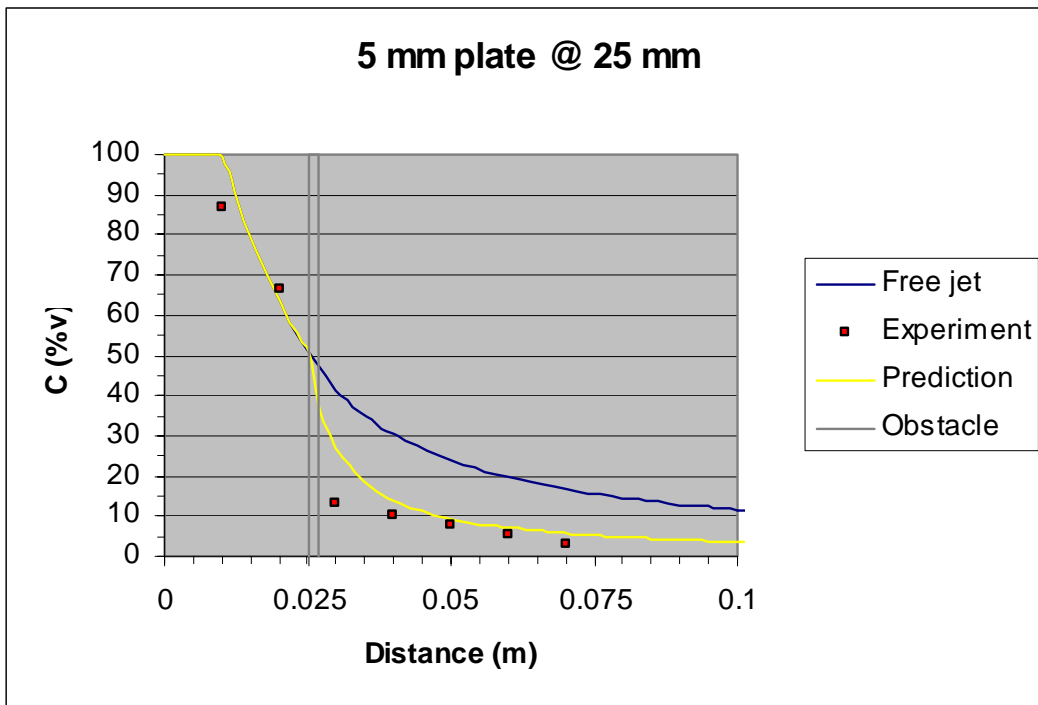


Figure 14: Concentration as function of downstream distance for jet hitting 5 mm flat obstacle at distance of 25 mm

This test shows a much more dramatic drop in concentration downstream of the obstacle than was observed for cylindrical obstacles. Good agreement with the model is found once the effect of obstacle drag coefficient in Equation (24) has been calibrated. In Figure 15, the same flat plate was positioned at 50 mm from the release point and the effects of the obstacle are much less marked, but are still well predicted by the model.

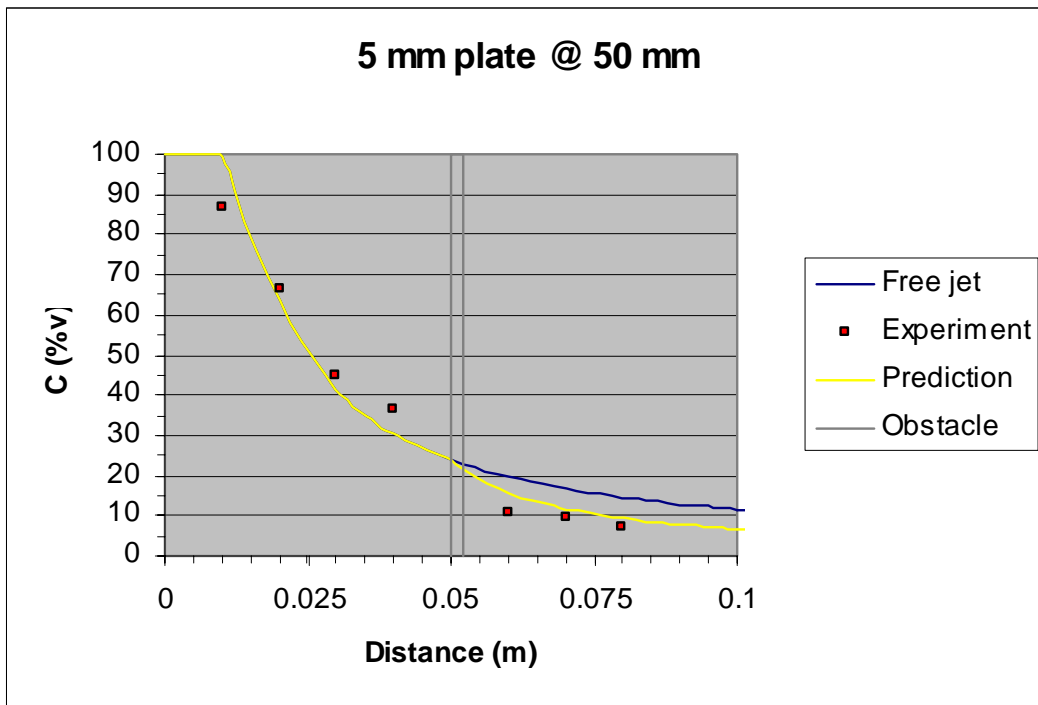


Figure 15: Concentration as function of downstream distance for jet hitting 5 mm flat obstacle at distance of 50 mm

4.3 JIP data

As part of a Joint Industry Project (JIP) on offshore gas build-up, Advantica has carried out a series of gas releases in a full-scale representation of an offshore module [4]. Figures 16 and 17 show external and internal views of the experimental rig. Although the tests were primarily designed to monitor the build-up of gas within the bulk atmosphere of the module, some releases were directed from a 43 mm diameter nozzle onto a cylindrical obstacle using a range of release rates and in a small range of low-windspeed conditions. The obstacle was positioned 2 m from the release point and was 2.9 m long with a diameter of 0.91 m. Figure 18 shows a representation of a section of the internal congestion with the impacted obstacle highlighted.



Figure 16: External view of full-scale rig used for Joint Industry Project on offshore gas build-up



Figure 17: Internal view of full-scale rig used for Joint Industry Project on offshore gas build-up

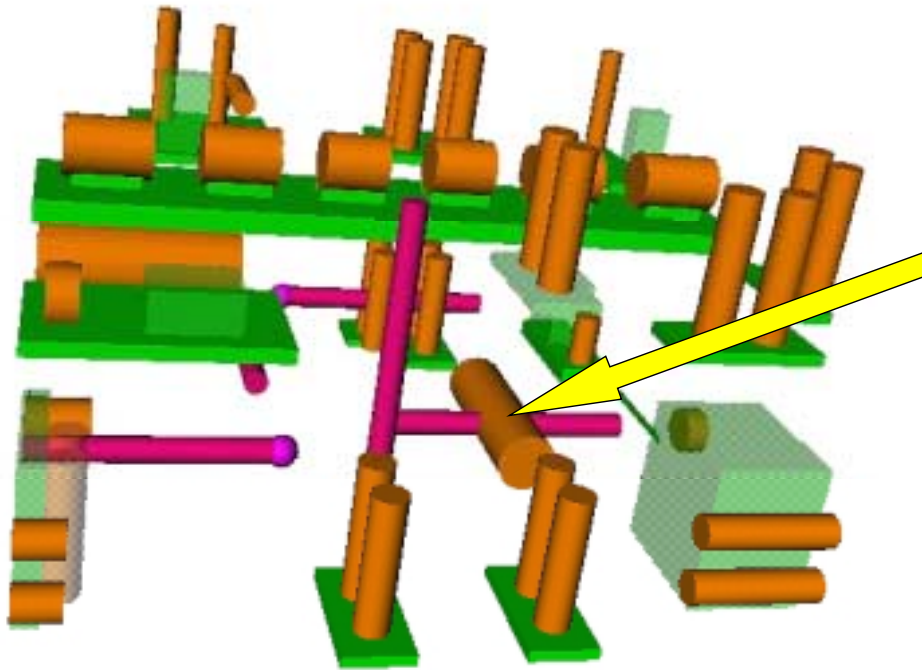


Figure 18: Schematic view of internal obstacle arrangement showing release directions used in tests (red markers), and obstacle used for jet impaction (arrowed)

Since the rig is quite highly confined and congested (and therefore restricts air movement), it is useful to check that the behaviour of those releases which did not interact with obstacles is correctly predicted by the free jet model. Any major discrepancy for these cases would mean that subsequent comparisons for obstacle interaction would yield little useful information on the performance of the model. Figure 19 shows the predicted and measured concentrations for an unimpeded test with a release directed directly downwind. Reasonably good agreement is demonstrated, so further comparisons with impeded jet tests should be worthwhile. Note that the predicted gas concentrations in all of these tests have been corrected for background gas build-up in the bulk atmosphere of the rig, since the jet is entraining some additional gas which will have augmented the measured concentration values. The correction factor applied to the predicted concentration levels was calculated as follows:

$$C_{corr} = C_{pred} + (1 - C_{pred}) \cdot C_{bulk} \quad (20)$$

For the free jet comparison, there was no background gas build-up, so no correction factor was applied.

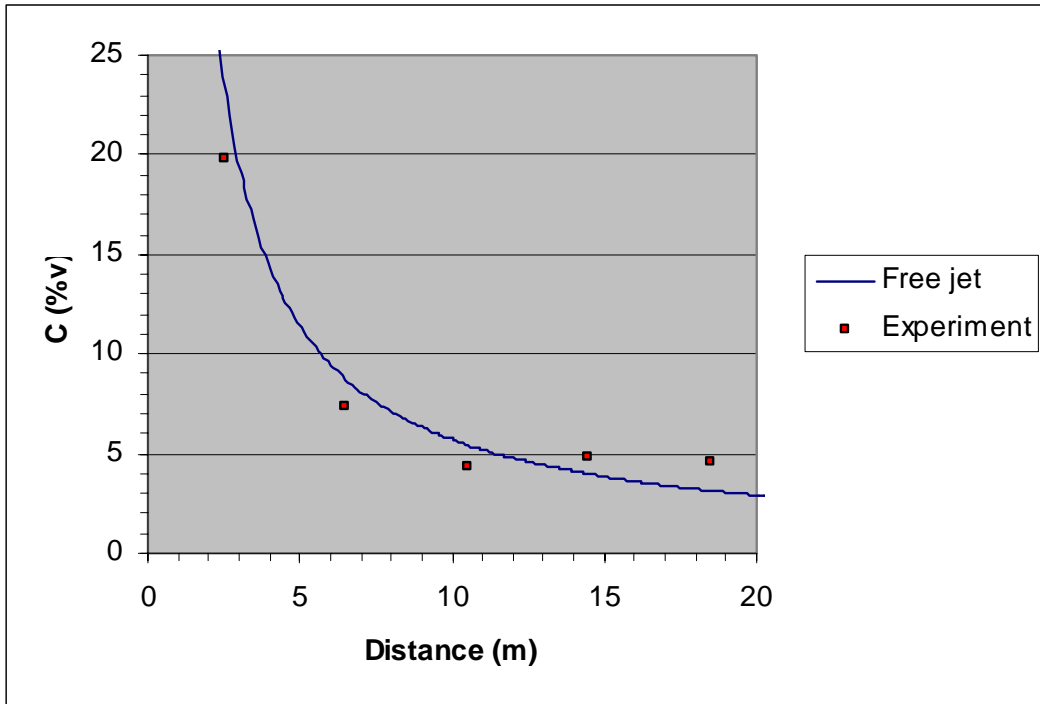


Figure 19: Concentration as function of downstream distance for free jet directed downwind (background concentration 0 %)

Figures 20 to 24 show comparisons of predicted and measured concentrations for the tests in which the jet was impeded by the cylindrical obstacle, at a number of different release rates and in different wind-speeds.

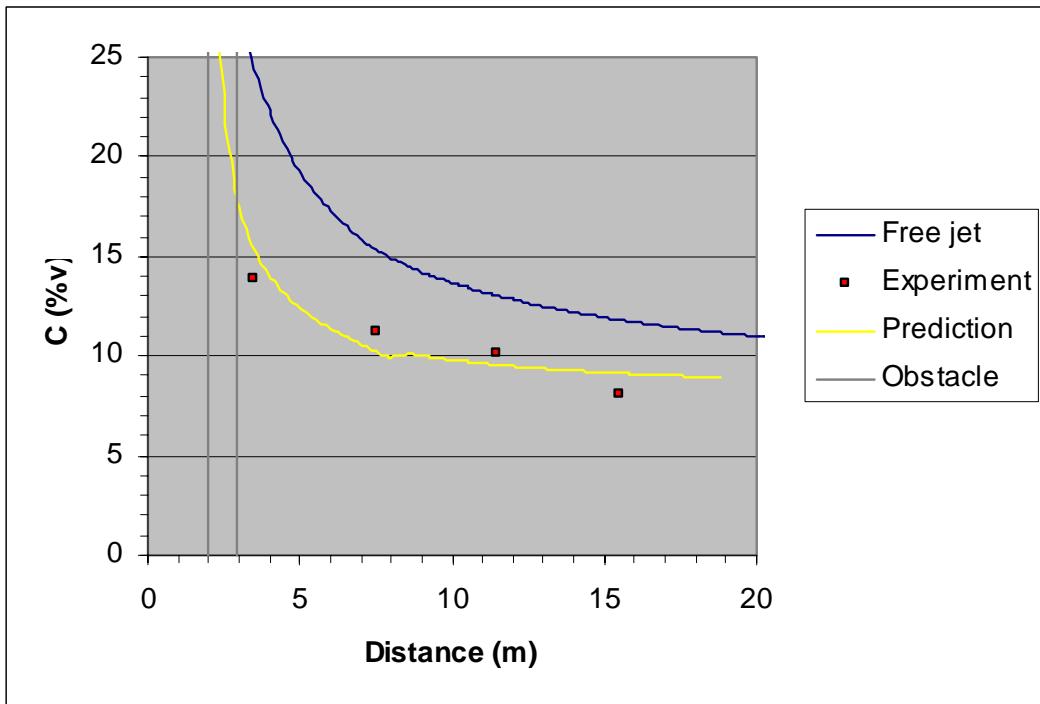


Figure 20: Concentration as function of downstream distance for impeded jet directed upwind (background concentration 8 %)

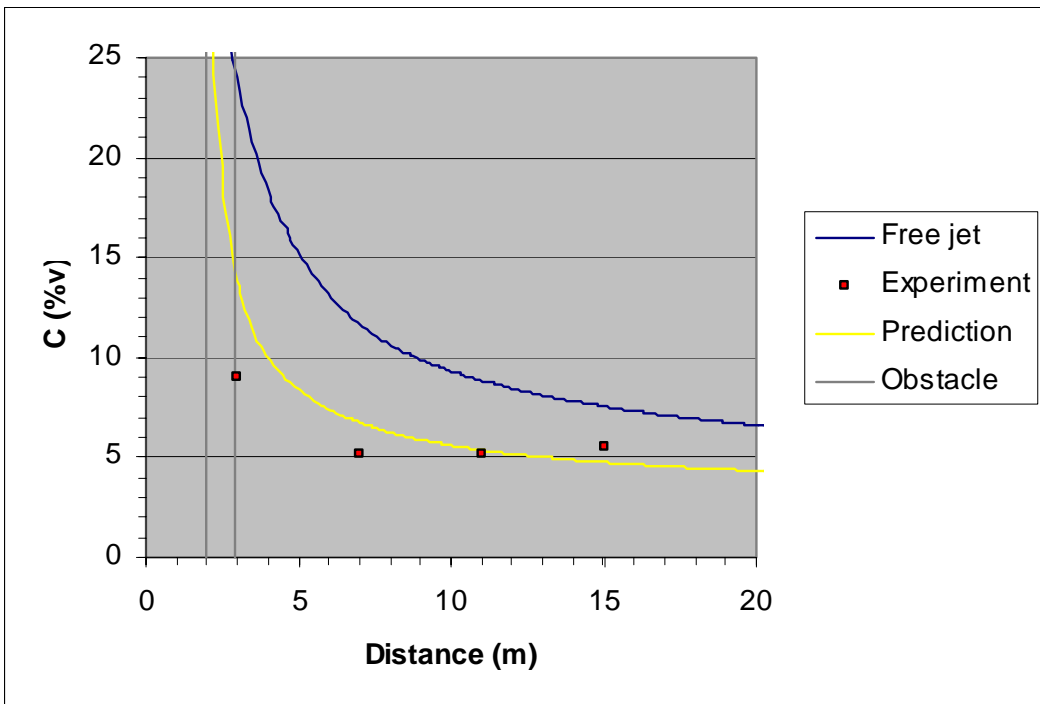


Figure 21: Concentration as function of downstream distance for impeded jet directed downwind (background concentration 3 %)

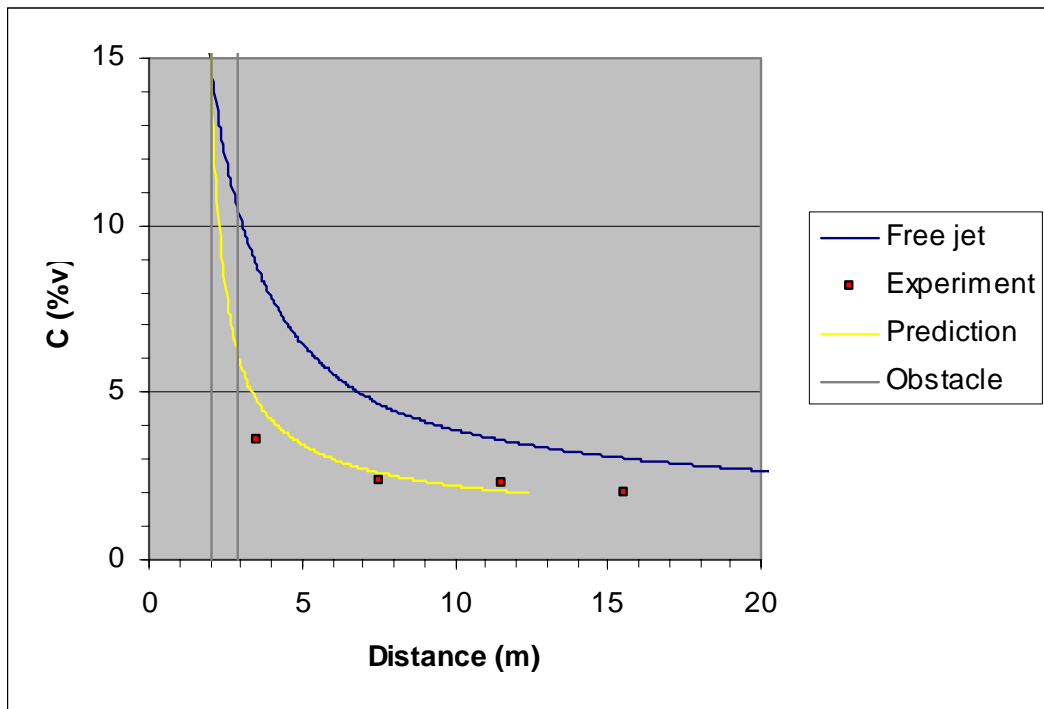


Figure 22: Concentration as function of downstream distance for impeded jet directed downwind (background concentration 1 %)

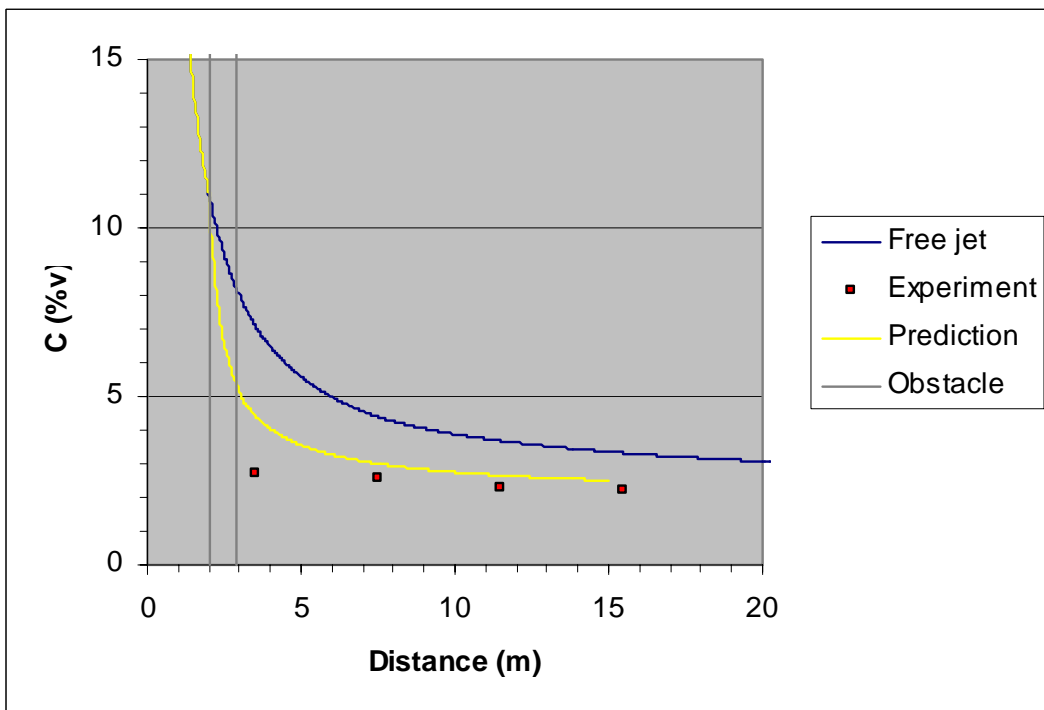


Figure 23: Concentration as function of downstream distance for impeded jet directed downwind (background concentration 2 %)

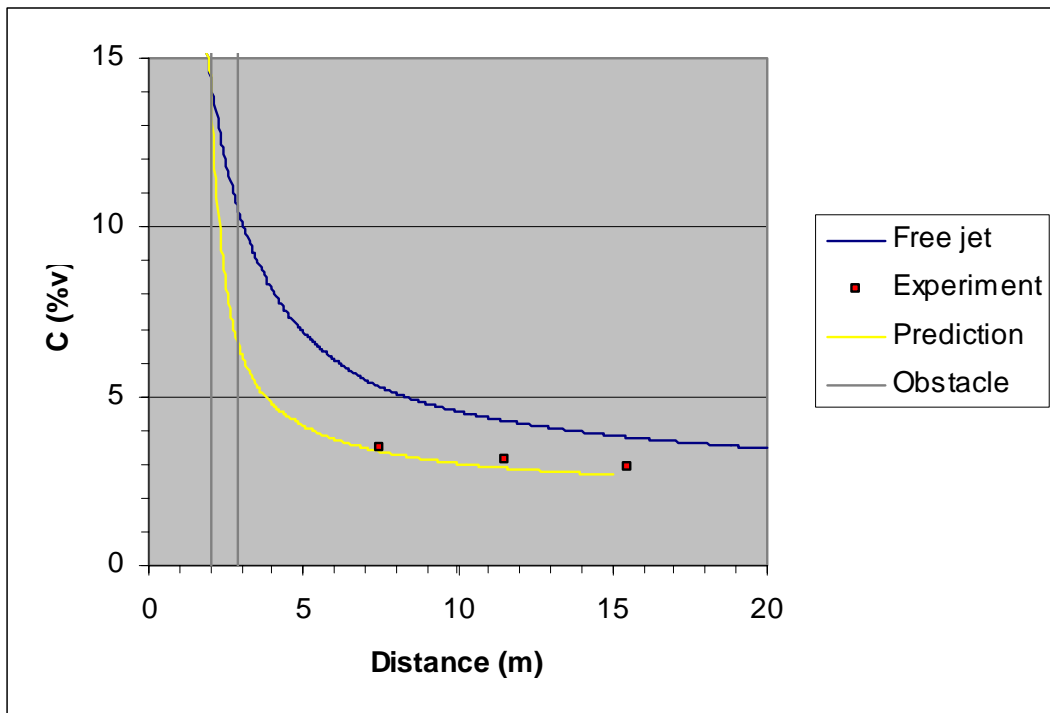


Figure 24: Concentration as function of downstream distance for impeded jet directed downwind (background concentration 2 %)

All of these tests show excellent agreement with the model predictions with no further calibration or modification having been applied.

5 DISCUSSION

The results of the comparison of the model predictions with the available experimental data presented in Section 4 of this report have demonstrated that it is possible to use a relatively simple integral model to predict the bulk flow parameters associated with a high momentum gaseous jet interacting with simple obstacle configurations. However, the methodology proposed here does contain a number of sub-models that still require further validation or calibration using experimental data. In particular, these are:

1. Jet interaction with short obstacles whose length is of the same order as their diameter / width;
2. Interaction with obstacles at angles other than perpendicular to the obstacle;
3. Interaction with large (stopping) obstacles at an angle;
4. Interaction with multiple obstacles, e.g. successive cylinders with similar or dissimilar dimensions;
5. Interaction with obstacle arrays, such as pipe-work and the development of a composite obstacle type to represent such arrays as a single obstacle.

With further development, it is feasible that the techniques presented in this report could be extended to dispersing two-phase jet releases and jet fires.

6 REFERENCES

1. R.P. Cleaver and P.D. Edwards, *Comparison of an integral model for predicting the dispersion of a turbulent jet in a crossflow with experimental data*. Journal of Loss Prevention in the Process Industries, **3**, 91-96 (1990).
2. R.P. Cleaver, M.G. Cooper and D. Piper, *Gas dispersion and build-up within offshore modules*. Offshore Safety and Reliability, Safety and Reliability Symposium, Sutton Coldfield, UK (1991)
3. S.G. Bryce and R.E.J. Fryer-Taylor, *Flow structure and mixing in obstructed and confined jets*. Eighth Symposium on Turbulent Shear Flows, Technical University of Munich, 14-2 (1991).
4. C. Savvides, V. Tam, R.P. Cleaver, S. Darby, G.Y. Buss, R.E. Britter and S. Connolly, *Gas dispersion in a congested, partially confined volume*. International Conference and Workshop on Modelling the Consequences of Accidental Releases of Hazardous Materials, Sept. 1999, San Francisco. A.I.Ch.E. (1999).

NOMENCLATURE

c_M	Bulk mass fraction of fuel in jet [-]
C_{bulk}	Volume fraction of fuel in bulk atmosphere [-]
C_{corr}	Volume fraction of fuel in jet, corrected for background level [-]
C_{pred}	Volume fraction of fuel in jet as predicted by model [-]
D_X	Drag in x direction [kg/s^2]
D_Y	Drag in y direction [kg/s^2]
E	Air entrainment rate into jet [kg/m s]
E_1	Air entrainment rate due to shear [kg/m s]
E_2	Air entrainment rate due to buoyancy [kg/m s]
E_3	Air entrainment rate due to atmospheric turbulence [kg/m s]
g	Acceleration due to gravity [m/s^2]
H	Jet specific enthalpy [J/kg]
H_∞	Ambient specific enthalpy [J/kg]
LFL	Lower flammable limit
\dot{M}	Total mass flux in jet [kg/s]
R	Jet bulk radius [m]
s	Distance along jet centreline [m]
U_∞	Ambient wind speed at jet height [m/s]
W	Total momentum [$\text{kg m}^2/\text{s}^2$]
W_H	Horizontal momentum [$\text{kg m}^2/\text{s}^2$]
W_V	Vertical momentum [$\text{kg m}^2/\text{s}^2$]
W_X	Horizontal momentum in x direction [$\text{kg m}^2/\text{s}^2$]
W_Y	Horizontal momentum in y direction [$\text{kg m}^2/\text{s}^2$]
W_∞	Ambient momentum in jet direction [$\text{kg m}^2/\text{s}^2$]
$\alpha_{1,2,3}$	Entrainment coefficients [-]
ϕ	Jet angle in vertical plane (measured from downwind) [r]
ψ	Jet angle in horizontal plane (measured from downwind) [r]

ν_{∞}	Ambient turbulent viscosity [m^2/s]
ρ	Jet bulk density [kg/m^3]
ρ_{∞}	Ambient density [kg/m^3]

A Appendix – User guide

The JINX jet dispersion model [1] is a PC-based application written in FORTRAN that can be run either interactively or directly from data files. Typical run times are of the order of a few seconds. The first part of this appendix describes each of the input parameters, whether entered interactively or from a data file. The subsequent sections describe the format of the data input file for obstacles together with sample input and output files.

A1 : Running JINX

The following data is required by the program and may be entered interactively via the keyboard or from a re-run file. Note that not all of the inputs are required for every run – some parameters are only required depending on other values that have been entered.

Output file – The name of the ASCII text file to which output will be written.

Title – A short descriptive title for the run that will appear at the top of the output file.

Stack height – The height of the release point (m) above ground level.

Release diameter – The internal diameter of the orifice at the exit point (m). If the release is sonic, the program will automatically calculate a pseudo-diameter.

Discharge coefficient – The discharge coefficient at the orifice. A value of 0.86 is normally appropriate for a smooth, straight pipe under sub-sonic conditions, or 1.0 for sonic conditions. Rough or non-circular exits may have lower coefficients.

Release angle from horizontal – The angle of the release measured upwards from the horizontal plane (degrees). Zero degrees is horizontal, 90 degrees is vertical.

Release angle from downwind – The angle of the release measured anti-clockwise (looking from above) from the downwind direction. Zero degrees is downwind, 90 degrees is at right angles to the wind, 180 degrees is upwind.

Release rate – The total mass release rate through the orifice (kg/s). The release is assumed to be at a concentration of 100% at the orifice.

Molecular weight of gas – The mean molecular weight (g/mol) of the released material.

Specific heat of gas – The specific heat at constant pressure of the released material (J/kg.K). The model uses a constant value, so a mean figure, averaged over the temperature range to be considered should be entered.

Ratio of specific heats of gas – The ratio of the specific heat at constant pressure to the value at constant volume (“gamma”). This is a function of

pressure, so account should be taken for this if releases are from high stagnation pressures.

Gas temperature – The stagnation temperature (K) in the reservoir, or upstream of the orifice.

Averaging time – Specify short ('S') or long ('L') term averaging. Short term averaging should be used for flammable or lethally toxic releases, where short duration peak concentrations define the hazard. Long term averaging should be selected only for mildly toxic releases – this will predict lower concentrations, averaged over longer time scales.

Wind speed – The reference wind speed (m/s) at the specified wind speed height. This speed is constant for plug flow conditions, but will be a function of height if a boundary layer profile is used.

Wind speed height – The reference height above ground level (m) at which the input wind speed applies. This is unimportant for plug flows, but a valid figure should still be entered.

Pasquill stability category – The type of atmospheric stability category to be specified. For boundary layer profiles, the letters 'A' to 'F' may be entered. 'A' to 'C' correspond to unstable conditions, 'D' is neutral and 'E' and 'F' are for stable conditions. Entering 'P' will select a plug flow, with the wind speed and temperature being independent of height. 'P' must be selected if using a zero wind speed, but should not otherwise be used to represent a normal outdoor situation.

Surface roughness – The aerodynamic surface roughness length (m). This is used to generate the boundary layer profiles. Typical values are 10^{-4} m for flat sea, 5×10^{-3} to 2×10^{-2} m for grassed areas, 2×10^{-2} to 0.1m for rural terrain and between 0.1 and 0.3m for urban areas.

Turbulence intensity – The turbulence intensity of the atmospheric cross-flow (%), defined as the ratio of the fluctuations in flow velocity to the mean flow velocity. This is selected for 'plug' flows only. A low intensity would be about 1%; 5 to 15% might correspond to areas close to the ground. (Note: this input is ignored for zero wind speeds, but a value is still required).

Molecular weight of air – The molecular weight of the ambient air (g/mol). (Typically 29.96).

Specific heat of air – The specific heat at constant pressure for the ambient air (J/kg.K). (Typically 993.0).

Air temperature – The atmospheric temperature (K). This is a function of height for boundary layer profiles in non-neutral stability.

Atmospheric pressure – The ambient pressure (bar). (Typically 1.01325).

Number of diameters between outputs – The output step length, based on the initial diameter (or pseudo-diameter for sonic releases). Enter an integer

number of one or greater. This selection does not impair the efficiency or accuracy of the internal calculations.

Stopping concentration – The limiting centreline concentration (vol %) at which execution of the program will stop. (Typically the LFL of the released material).

A2 : Using obstacles

The layout of obstacles is specified in an ASCII text file, whether JINX is run interactively or from a re-run file. As currently implemented, the obstacle data file must be named 'OBS.DAT' and reside in the folder from which JINX is being run. If no such file is found, the program assumes that no obstacles are required.

The first line of the data file contains the number of obstacles to be read from the file. This enables the user to ignore some (or all) of the obstacles without actually deleting them from the file.

Each subsequent line contains data for one obstacle. An obstacle is described by seven parameters as follows:

X0 – The obstacle start position (m) in the x (downwind) direction, measured from the release point.

Y0 – The obstacle start position (m) in the y (crosswind) direction, measured from the release point.

Z0 – The obstacle start position (m) in the z (vertical) direction, measured upwards from the ground.

Angle – the orientation of the obstacle (degrees) measured anti-clockwise (looking from above) from the downwind direction. Ignored for vertical obstacles, but a value is still required.

D – The diameter or width of the obstacle (m).

L – The length of the obstacle (m).

Type – An integer describing the obstacle type. At present, the following obstacle types are defined:

1 – Horizontal cylinder

2 – Horizontal box

101 – Vertical cylinder

102 – Vertical box

Note that since the obstacle interaction model is not a 'finished' product, it has one or two minor quirks which the user should be aware of. In particular, it will be apparent that it is possible to specify horizontal obstacles in either of two ways, i.e. using

either end of the obstacle as the origin. The origin for these obstacles should be chosen such that they run in an anti-clockwise direction (as seen from above) from their origin about the release point. Failure to observe this may result in the jet failing to interact with them.

An example of an obstacle data file is listed in Section A3.

A3 : Sample input files

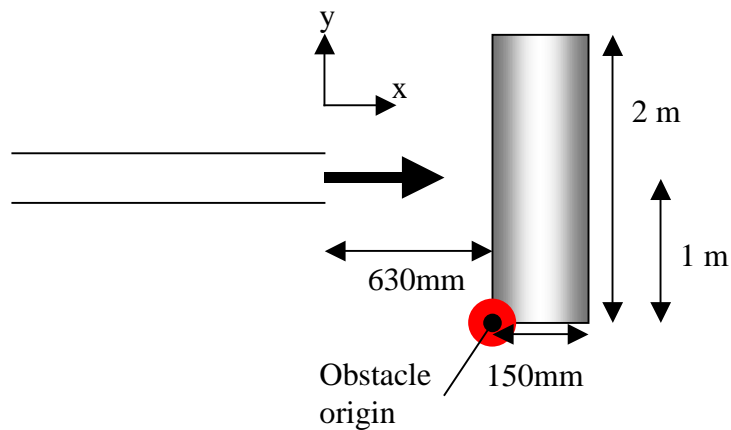
Reproduced below is the JINX input file used to produce the data in Figure 9 of the main report.

```
This file is for input to JINX V2.0
150b.out
150 mm obstacle at 630mm
 1.0000      !Stack height (m)
0.01070     !Release Diameter (m)
 1.0000     !Discharge Coefficient
 0.         !Release angle to horizontal (deg)
 0.         !Release angle from d/w (deg)
0.011      !Release Rate (kg/s)
 18.200     !Molecular weight (kg/kMol)
 1972.0     !Specific heat capacity of gas (J/kg/°K)
 1.3400     !Ratio of specific heats of gas
 288.15     !Temperature of gas (K)
S          !Type of averaging
 0.0001     !Wind speed (m/s)
 10.000     !Wind speed height (m)
D          !Pasquill stability category
0.00010    !Surface roughness (m)
 28.960     !Molecular weight of air (kg/kMol)
 993.00     !Specific heat capacity of air (J/kg/K)
 283.00     !Air temperature (°K)
 1.01325    !Atmospheric pressure (Bar)
           1 !Number of diameters between outputs
 2.5000     !Stopping concentration (mol%)
```

Below is the obstacle data file 'OBS.DAT' use for the same simulation.

```
1
0.630 -1.0 1.0 90. 0.150 2.0 1
```

This data corresponds to the configuration shown below:



A4 : Output file

JINX produces output in the form of an ASCII text file. At the top of the output file, JINX reproduces the input data and some computed values related to the flow which may be of interest to the user. Most of these are self-explanatory, but the “wind profile index”, n , is the exponent used to evaluate the wind speed at any height:

$$U = U_{ref} \left(Z / Z_{ref} \right)^n$$
 where n is calculated from the supplied atmospheric stability and surface roughness.

Finally, JINX prints the results of the simulation as twelve columns of data that are explained below.

Col.1 – Downwind distance (m) from the release point.

Col.2 – Crosswind distance (m) from the release point.

Col.3 – Vertical distance (m) above the ground.

Col.4 – Distance from the release point (m) measured along the jet trajectory.

Col.5 – Current trajectory angle above horizontal (deg).

Col.6 – Current trajectory angle measured anti-clockwise from downwind direction (deg).

Col.7 – Concentration (% vol.) of released material on the jet centreline.

Col.8 – Gas velocity (m/s) on the jet centreline.

Col.9 – Temperature (K) on the jet centreline.

Col.10 – Jet radius (m) to zero concentration.

Col.11 – Time of flight (s) from the release point.

Col.12 – Various flags giving feedback on the model performance.

The output of JINX corresponding to the input files listed in Section A3 is reproduced on the following pages.

150 mm obstacle at 630mm

Stack

Stack height 1.000 m
 Vert.Release angle 0.00 deg
 Hor. Release angle 0.00 deg
 Orifice diameter 0.10700E-01 m
 Discharge coeff. 1.0000

Release

Release is subsonic
 Mach number 0.37398
 Mass flux 0.11000E-01 Kg/s
 Molecular weight 18.200 Kg/Kmol
 Specific heat Cp 1972.0 J/(Kg K)
 Ratio of specific heats 1.3400
 Density (at 283.K) 0.78375 Kg/m^3
 Upstream temperature 288.15 K
 Momentum flux 1.7076 Kg m/s^2
 Bulk exit velocity 155.23 m/s

Atmosphere

Wind speed at 10 m 0.10000E-03 m/s
 Molecular weight 28.960 Kg/Kmol
 Specific heat Cp 993.00 J/(Kg K)
 Density (at 283.K) 1.2471 Kg/m^3
 Ground temperature 283.00 K
 Pressure 1.01325 bars
 Wind profile index 0.80521E-01
 Surface roughness length 0.10000E-03 m
 Stability category D

Other values

Type of time averaging S
 Jet to wind velocity ratio 0.18686E+07
 Output step length 0.10700E-01 m
 Output printed every 1 diameters
 Stopping volume percent 2.500 %

x (m)	y (m)	z (m)	s (m)	phi (deg)	psi (deg)	vol fr. (%)	Ujet (m/s)	temp (K)	radius (m)	time (s)	
0.00	0.00	1.00	0.00	0.0	0.0	100.000	155.23	290.7	0.01	0.00	CO VO
0.107E-01	0.00	1.00	0.107E-01	0.0	0.0	100.000	155.23	290.4	0.01	.723E-04	CO VO
0.214E-01	0.00	1.00	0.214E-01	0.0	0.0	100.000	155.23	290.0	0.01	.152E-03	CO VO
0.321E-01	0.00	1.00	0.321E-01	0.0	0.0	100.000	155.23	289.7	0.01	.239E-03	CO VO
0.428E-01	0.00	1.00	0.428E-01	0.0	0.0	100.000	155.23	289.3	0.01	.336E-03	CO VO
0.535E-01	0.00	1.00	0.535E-01	0.0	0.0	100.000	155.23	289.0	0.01	.442E-03	CO VO
0.642E-01	0.00	1.00	0.642E-01	0.0	0.0	100.000	155.23	288.6	0.01	.558E-03	CO VO
0.749E-01	0.00	1.00	0.749E-01	0.0	0.0	96.464	145.34	288.3	0.01	.686E-03	
0.856E-01	0.00	1.00	0.856E-01	0.0	0.0	89.588	131.47	288.0	0.01	.827E-03	
0.963E-01	0.00	1.00	0.963E-01	0.0	0.0	83.074	118.97	287.7	0.02	.982E-03	
0.107	0.00	1.00	0.107	0.0	0.0	76.922	107.71	287.4	0.02	.115E-02	
0.118	0.00	1.00	0.118	0.0	0.0	71.128	97.56	287.1	0.02	.134E-02	
0.128	0.00	1.00	0.128	0.0	0.0	65.686	88.39	286.8	0.02	.155E-02	
0.139	0.00	1.00	0.139	0.0	0.0	60.587	80.11	286.6	0.02	.177E-02	
0.150	0.00	1.00	0.150	0.0	0.0	55.836	72.65	286.3	0.02	.202E-02	
0.160	0.00	1.00	0.160	0.0	0.0	51.679	66.31	286.1	0.03	.230E-02	
0.171	0.00	1.00	0.171	0.0	0.0	48.098	60.99	285.9	0.03	.259E-02	
0.182	0.00	1.00	0.182	0.0	0.0	44.982	56.47	285.8	0.03	.292E-02	
0.193	0.00	1.00	0.193	0.0	0.0	42.245	52.56	285.6	0.03	.326E-02	
0.203	0.00	1.00	0.203	0.0	0.0	39.821	49.16	285.5	0.03	.363E-02	
0.214	0.00	1.00	0.214	0.0	0.0	37.661	46.18	285.3	0.04	.403E-02	
0.225	0.00	1.00	0.225	0.0	0.0	35.722	43.53	285.2	0.04	.445E-02	
0.235	0.00	1.00	0.235	0.0	0.0	33.974	41.18	285.2	0.04	.489E-02	
0.246	0.00	1.00	0.246	0.0	0.0	32.389	39.06	285.0	0.04	.536E-02	
0.257	0.00	1.00	0.257	0.0	0.0	30.945	37.15	285.0	0.04	.585E-02	
0.267	0.00	1.00	0.267	0.0	0.0	29.625	35.42	284.9	0.05	.637E-02	
0.278	0.00	1.00	0.278	0.0	0.0	28.412	33.85	284.8	0.05	.691E-02	
0.289	0.00	1.00	0.289	0.0	0.0	27.295	32.40	284.7	0.05	.748E-02	
0.300	0.00	1.00	0.300	0.0	0.0	26.262	31.08	284.7	0.05	.807E-02	
0.310	0.00	1.00	0.310	0.0	0.0	25.305	29.86	284.6	0.06	.868E-02	
0.321	0.00	1.00	0.321	0.0	0.0	24.415	28.73	284.6	0.06	.932E-02	
0.332	0.00	1.00	0.332	0.0	0.0	23.585	27.69	284.6	0.06	.998E-02	
0.342	0.00	1.00	0.342	0.0	0.0	22.810	26.71	284.5	0.06	.107E-01	
0.353	0.00	1.00	0.353	0.0	0.0	22.085	25.81	284.4	0.06	.114E-01	
0.364	0.00	1.00	0.364	0.0	0.0	21.404	24.96	284.4	0.07	.121E-01	
0.374	0.00	1.00	0.374	0.0	0.0	20.763	24.17	284.3	0.07	.129E-01	
0.385	0.00	1.00	0.385	0.0	0.0	20.160	23.42	284.3	0.07	.137E-01	
0.396	0.00	1.00	0.396	0.0	0.0	19.591	22.72	284.3	0.07	.145E-01	
0.407	0.00	1.00	0.407	0.0	0.0	19.054	22.06	284.3	0.07	.153E-01	
0.417	0.00	1.00	0.417	0.0	0.0	18.545	21.44	284.3	0.08	.162E-01	

0.428	0.00	1.00	0.428	0.0	0.0	18.062	20.85	284.2	0.08	.170E-01
0.439	0.00	1.00	0.439	0.0	0.0	17.604	20.30	284.2	0.08	.179E-01
0.449	0.00	1.00	0.449	0.0	0.0	17.169	19.77	284.1	0.08	.189E-01
0.460	0.00	1.00	0.460	0.0	0.0	16.754	19.27	284.1	0.08	.198E-01
0.471	0.00	1.00	0.471	0.0	0.0	16.359	18.79	284.1	0.09	.208E-01
0.481	0.00	1.00	0.481	0.0	0.0	15.982	18.34	284.0	0.09	.218E-01
0.492	0.00	1.00	0.492	0.1	0.0	15.623	17.91	284.0	0.09	.228E-01
0.503	0.00	1.00	0.503	0.1	0.0	15.279	17.49	284.0	0.09	.239E-01
0.514	0.00	1.00	0.514	0.1	0.0	14.950	17.10	284.0	0.10	.250E-01
0.524	0.00	1.00	0.524	0.1	0.0	14.635	16.72	284.0	0.10	.261E-01
0.535	0.00	1.00	0.535	0.1	0.0	14.333	16.36	284.0	0.10	.272E-01
0.546	0.00	1.00	0.546	0.1	0.0	14.043	16.02	284.0	0.10	.283E-01
0.556	0.00	1.00	0.556	0.1	0.0	13.764	15.69	283.9	0.10	.295E-01
0.567	0.00	1.00	0.567	0.1	0.0	13.496	15.37	283.9	0.11	.307E-01
0.578	0.00	1.00	0.578	0.1	0.0	13.239	15.07	283.9	0.11	.319E-01
x	y	z	s	phi	psi	vol fr.	Ujet	temp	radius	time
(m)	(m)	(m)	(m)	(deg)	(deg)	(%)	(m/s)	(K)	(m)	(s)
0.588	0.00	1.00	0.588	0.1	0.0	12.991	14.77	283.9	0.11	.332E-01
0.599	0.00	1.00	0.599	0.1	0.0	12.753	14.49	283.9	0.11	.344E-01
0.610	0.00	1.00	0.610	0.1	0.0	12.523	14.22	283.9	0.11	.357E-01
0.621	0.00	1.00	0.621	0.1	0.0	12.301	13.96	283.8	0.12	.370E-01

NOTE : The release has hit obstacle 1

0.630	0.00	1.00	0.630	0.1	0.0	12.112	11.75	283.8	0.13	.382E-01
0.641	0.00	1.00	0.641	0.1	0.0	11.573	11.21	283.8	0.13	.398E-01
0.651	0.00	1.00	0.651	0.1	0.0	11.080	10.72	283.7	0.14	.415E-01
0.662	0.00	1.00	0.662	0.1	0.0	10.628	10.27	283.7	0.15	.433E-01
0.673	0.00	1.00	0.673	0.1	0.0	10.211	9.85	283.7	0.15	.452E-01
0.684	0.00	1.00	0.684	0.1	0.0	9.825	9.47	283.7	0.16	.471E-01
0.694	0.00	1.00	0.694	0.1	0.0	9.468	9.11	283.7	0.16	.491E-01
0.705	0.00	1.00	0.705	0.1	0.0	9.135	8.79	283.6	0.17	.511E-01
0.716	0.00	1.00	0.716	0.1	0.0	8.825	8.48	283.6	0.18	.533E-01
0.726	0.00	1.00	0.726	0.1	0.0	8.536	8.20	283.6	0.18	.555E-01
0.737	0.00	1.00	0.737	0.1	0.0	8.265	7.93	283.6	0.19	.578E-01
0.748	0.00	1.00	0.748	0.1	0.0	8.010	7.68	283.6	0.19	.602E-01
0.758	0.00	1.00	0.758	0.2	0.0	7.771	7.44	283.6	0.20	.627E-01
0.769	0.00	1.00	0.769	0.2	0.0	7.546	7.22	283.5	0.21	.652E-01
0.780	0.00	1.00	0.780	0.2	0.0	7.333	7.02	283.5	0.21	.678E-01
0.791	0.00	1.00	0.791	0.2	0.0	7.132	6.82	283.5	0.22	.705E-01
0.801	0.00	1.00	0.801	0.2	0.0	6.942	6.63	283.5	0.22	.732E-01
0.812	0.00	1.00	0.812	0.2	0.0	6.761	6.46	283.5	0.23	.761E-01

0.823	0.00	1.00	0.823	0.2	0.0	6.590	6.29	283.5	0.24	.790E-01
0.833	0.00	1.00	0.833	0.2	0.0	6.427	6.13	283.4	0.24	.820E-01
0.844	0.00	1.00	0.844	0.2	0.0	6.272	5.98	283.4	0.25	.850E-01
0.855	0.00	1.00	0.855	0.2	0.0	6.125	5.84	283.4	0.25	.881E-01
0.865	0.00	1.00	0.865	0.2	0.0	5.984	5.70	283.4	0.26	.914E-01
0.876	0.00	1.00	0.876	0.2	0.0	5.849	5.57	283.4	0.27	.946E-01
0.887	0.00	1.00	0.887	0.2	0.0	5.721	5.45	283.4	0.27	.980E-01
0.898	0.00	1.00	0.898	0.3	0.0	5.598	5.33	283.4	0.28	.101
0.908	0.00	1.00	0.908	0.3	0.0	5.480	5.22	283.4	0.28	.105
0.919	0.00	1.00	0.919	0.3	0.0	5.367	5.11	283.4	0.29	.109
0.930	0.00	1.00	0.930	0.3	0.0	5.258	5.00	283.4	0.30	.112
0.940	0.00	1.00	0.940	0.3	0.0	5.154	4.90	283.4	0.30	.116
0.951	0.00	1.00	0.951	0.3	0.0	5.054	4.80	283.4	0.31	.120
0.962	0.00	1.00	0.962	0.3	0.0	4.958	4.71	283.3	0.31	.124
0.972	0.00	1.00	0.972	0.3	0.0	4.865	4.62	283.3	0.32	.128
0.983	0.00	1.00	0.983	0.3	0.0	4.776	4.54	283.3	0.33	.132
0.994	0.00	1.00	0.994	0.3	0.0	4.689	4.45	283.3	0.33	.136
1.00	0.00	1.00	1.00	0.4	0.0	4.606	4.37	283.3	0.34	.140
1.02	0.00	1.00	1.02	0.4	0.0	4.526	4.30	283.3	0.34	.144
1.03	0.00	1.00	1.03	0.4	0.0	4.449	4.22	283.3	0.35	.149
1.04	0.00	1.00	1.04	0.4	0.0	4.374	4.15	283.3	0.36	.153
1.05	0.00	1.00	1.05	0.4	0.0	4.302	4.08	283.3	0.36	.158
1.06	0.00	1.00	1.06	0.4	0.0	4.232	4.01	283.3	0.37	.162
1.07	0.00	1.00	1.07	0.4	0.0	4.164	3.95	283.3	0.37	.167
1.08	0.00	1.00	1.08	0.4	0.0	4.099	3.89	283.3	0.38	.171
1.09	0.00	1.00	1.09	0.5	0.0	4.035	3.82	283.3	0.39	.176
1.10	0.00	1.00	1.10	0.5	0.0	3.973	3.77	283.3	0.39	.181
1.11	0.00	1.00	1.11	0.5	0.0	3.914	3.71	283.3	0.40	.186
1.12	0.00	1.00	1.12	0.5	0.0	3.856	3.65	283.3	0.41	.191
1.13	0.00	1.00	1.13	0.5	0.0	3.799	3.60	283.3	0.41	.196
x	y	z	s	phi	psi	vol fr.	Ujet	temp	radius	time
(m)	(m)	(m)	(m)	(deg)	(deg)	(%)	(m/s)	(K)	(m)	(s)
1.14	0.00	1.00	1.14	0.5	0.0	3.745	3.55	283.3	0.42	.201
1.15	0.00	1.00	1.15	0.5	0.0	3.691	3.50	283.3	0.42	.207
1.16	0.00	1.00	1.17	0.6	0.0	3.640	3.45	283.3	0.43	.212
1.18	0.00	1.00	1.18	0.6	0.0	3.590	3.40	283.3	0.44	.217
1.19	0.00	1.00	1.19	0.6	0.0	3.541	3.35	283.3	0.44	.223
1.20	0.00	1.00	1.20	0.6	0.0	3.493	3.31	283.3	0.45	.228
1.21	0.00	1.00	1.21	0.6	0.0	3.447	3.26	283.3	0.45	.234
1.22	0.00	1.00	1.22	0.6	0.0	3.402	3.22	283.3	0.46	.240
1.23	0.00	1.00	1.23	0.6	0.0	3.358	3.18	283.3	0.47	.246
1.24	0.00	1.00	1.24	0.7	0.0	3.315	3.14	283.3	0.47	.251

1.25	0.00	1.00	1.25	0.7	0.0	3.273	3.10	283.3	0.48	.257
1.26	0.00	1.00	1.26	0.7	0.0	3.233	3.06	283.3	0.48	.263
1.27	0.00	1.00	1.27	0.7	0.0	3.193	3.02	283.3	0.49	.269
1.28	0.00	1.00	1.28	0.7	0.0	3.154	2.98	283.3	0.50	.276
1.29	0.00	1.00	1.29	0.7	0.0	3.117	2.95	283.2	0.50	.282
1.30	0.00	1.00	1.30	0.8	0.0	3.080	2.91	283.2	0.51	.288
1.31	0.00	1.00	1.31	0.8	0.0	3.044	2.88	283.2	0.51	.295
1.33	0.00	1.00	1.33	0.8	0.0	3.009	2.84	283.2	0.52	.301
1.34	0.00	1.00	1.34	0.8	0.0	2.974	2.81	283.2	0.53	.308
1.35	0.00	1.01	1.35	0.8	0.0	2.941	2.78	283.2	0.53	.314
1.36	0.00	1.01	1.36	0.8	0.0	2.908	2.75	283.2	0.54	.321
1.37	0.00	1.01	1.37	0.9	0.0	2.875	2.72	283.2	0.54	.328
1.38	0.00	1.01	1.38	0.9	0.0	2.844	2.69	283.2	0.55	.335
1.39	0.00	1.01	1.39	0.9	0.0	2.813	2.66	283.2	0.56	.341
1.40	0.00	1.01	1.40	0.9	0.0	2.783	2.63	283.2	0.56	.348
1.41	0.00	1.01	1.41	0.9	0.0	2.754	2.60	283.2	0.57	.356
1.42	0.00	1.01	1.42	1.0	0.0	2.725	2.57	283.2	0.57	.363
1.43	0.00	1.01	1.43	1.0	0.0	2.697	2.55	283.2	0.58	.370
1.44	0.00	1.01	1.44	1.0	0.0	2.669	2.52	283.2	0.59	.377
1.45	0.00	1.01	1.45	1.0	0.0	2.642	2.49	283.2	0.59	.385
1.46	0.00	1.01	1.46	1.0	0.0	2.615	2.47	283.2	0.60	.392
1.48	0.00	1.01	1.48	1.1	0.0	2.589	2.44	283.2	0.60	.400
1.49	0.00	1.01	1.49	1.1	0.0	2.564	2.42	283.2	0.61	.407
1.50	0.00	1.01	1.50	1.1	0.0	2.539	2.40	283.2	0.62	.415
1.51	0.00	1.01	1.51	1.1	0.0	2.514	2.37	283.2	0.62	.423
1.52	0.00	1.01	1.52	1.1	0.0	2.490	2.35	283.2	0.63	.430

STOP-Centreline concentration drops below specified value



MAIL ORDER

HSE priced and free
publications are
available from:

HSE Books
PO Box 1999
Sudbury
Suffolk CO10 2WA
Tel: 01787 881165
Fax: 01787 313995
Website: www.hsebooks.co.uk

RETAIL

HSE priced publications
are available from booksellers

HEALTH AND SAFETY INFORMATION

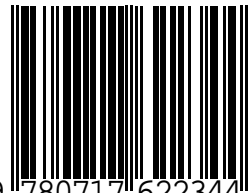
HSE InfoLine
Tel: 08701 545500
Fax: 02920 859260
e-mail: hseinformationservices@natbrit.com
or write to:
HSE Information Services
Caerphilly Business Park
Caerphilly CF83 3GG

HSE website: www.hse.gov.uk

CRR 396

£20.00

ISBN 0-7176-2234-7



9 780717 622344